Engineering Structures 148 (2017) 552–570

Contents lists available at ScienceDirect

Engineering Structures

journal homepage: www.elsevier.com/locate/engstruct

Estimating number of simultaneously yielding stories in a shear building subjected to earthquake excitation

Lisa Shrestha [a,1,*], Michel Bruneau [b]

[a] Earthquake Engineering Research and Consultation Center, Kathmandu, Nepal
[b] Dept. of Civil, Structural and Environmental Engineering, University at Buffalo, The State University of New York Buffalo, New York, USA

ARTICLE INFO

Article history:
Received 10 January 2017
Revised 5 May 2017
Accepted 17 June 2017

Keywords:
Simultaneous story yielding
Column design
Axial force
Earthquake excitation
Pulse excitation
Shear building
Multistory buildings

ABSTRACT

A procedure for estimating the number of simultaneously yielding stories (N_{SYS}) in a shear type building subjected to seismic ground excitation is proposed. Proper estimation of N_{SYS} values will lead to more accurate estimation of axial force demand in columns which will result in economical design of columns. In this procedure, the main pulse of the velocity record responsible for causing the maximum number of stories to yield simultaneously was identified and isolated to idealize it by a full-sine velocity pulse, as an extension of the procedure for estimating the N_{SYS} for a full-sine pulse velocity base excitation developed previously by the authors. A set of eighteen earthquake records sorted into three categories of earthquakes were considered, namely: earthquake excitations having (i) a single dominant pulse (ii) multiple distinct pulses, and; (iii) no distinct pulses in their velocity record. Since most of these earthquakes have relatively long duration main pulses, another set of eighteen earthquake records was obtained by condensing their acceleration time scale and was used to study the proposed procedure for earthquakes that have shorter duration main pulses. The estimated maximum value of N_{SYS} obtained from the proposed procedure was found to be adequately close to the actual value observed from OpenSees analysis for the structures and earthquakes considered.

1. Introduction

To achieve an economical design of columns in lateral-load-resisting systems, it is desirable to estimate the number of simultaneously yielding stories (N_{SYS}) as this directly impacts the axial force demands in columns (particularly given that such forces are currently often specified considering that all stories are yielding). In absence of proper estimation of the number of simultaneously yielding stories and hence axial force demand in columns, the capacity-design approach as implemented in current design procedures could severely overestimate the actual axial force demands on columns, resulting in overdesigned and economically inefficient columns. In an attempt to derive a systematic procedure for estimating the number of simultaneously yielding stories and use it to find axial force demand in columns of shear-buildings subjected to ground excitation (other than by empirically analyzing a large number of archetype structures), three essential steps were envisioned: First, a procedure must be developed for estimating the number of simultaneously yielding stories in a simple shear building subjected to velocity-pulse base excitation; Second, this procedure must be adapted as necessary for shear buildings subjected to actual earthquake excitations, in the perspective that earthquakes can be represented as a series of pulses, and; Third, a procedure must be formulated to estimate the axial force demand in columns considering the vertical force transferred from the simultaneously yielding stories and the other non-yielded stories above the column under consideration. The first step of the procedure that is focused on pulse-base excitations was presented in Shrestha and Bruneau [1].

The research work presented here focuses on the second of the above listed steps which is: investigation of a proposed procedure to estimate the N_{SYS} values for a shear building subjected to earthquake excitations, developed by extending the previous procedure for full-sine pulse velocity base excitation. The proposed procedure postulates that the maximum number of stories yielding simultaneously due to an earthquake excitation could be caused by the biggest pulse in its velocity record (an assumption based on observations from response to selected individual earthquake records). Accordingly, in the proposed procedure, the main pulse of the velocity record is isolated and idealized by a full-sine pulse, so that

* Corresponding author.
E-mail addresses: lisashre@buffalo.edu (L. Shrestha), bruneau@buffalo.edu (M. Bruneau).
[1] Formerly Graduate Research Assistant, Dept. of Civil, Structural and Environmental Engineering, University at Buffalo, Buffalo, NY 14260, USA.

http://dx.doi.org/10.1016/j.engstruct.2017.06.044

the estimation procedure developed previously for full-sine pulse base excitation could be applied.

The idea of representing ground motions either by equivalent pulses, series of equivalent pulses, or dominant pulses, has been around for decades. Techniques for representing near fault pulses vary from use of simple pulses like rectangular, triangular, trigonometric (sine, cosine) functions to more advanced techniques that uses wavelet analysis. Early procedures considered simulating earthquake excitations using simple pulse shapes (e.g. Hall et. al. [2]; Bruneau and Wang [3], [4]). Some recent works considered more advanced techniques for simulating and extracting the near fault pulse of the earthquake record. Based on wavelet analysis, Mavroeidis and Papageorgiou [5] used a modified form of Gabor wavelet to propose a step-by-step procedure to define amplitude A, frequency f_p (or pulse duration T_p), phase ν, and oscillatory character γ as needed parameters to represent near field ground motion. Baker [6] presented a method to classify a ground motion as "pulse-like" or "non-pulselike". Wavelet analysis using Daubechies wavelet was adopted in his procedure. Vassiliou and Makris [7] conducted wavelet analysis to extract the most energetic pulse from the acceleration record of an earthquake. Different types of wavelets were used in their work, including a cosine type B cycloidal pulse, a symmetric Ricker wavelet, an Antisymmetric Ricker wavelet, a Type C1 cycloidal pulse, a Type C2 cycloidal pulse, a Gabor wavelet modified by Mavroeidis and Papageorgiou [5] and referred to as the M&P wavelet, and a time derivative of the Gabor signal.

Here, a simple approach is used: in the proposed procedure, the main pulse in the velocity record responsible for causing the maximum number of stories yielding simultaneously is used and the use of a simple full-sine pulse for idealizing this main pulse was observed in many instances to be sufficient for the intended purpose. Simple pulse models, such as the sinusoidal pulses used by Kalkan and Kunnath [8], the triangular wave trains used by Krishnan and Muto [9], and other similar simple pulses, have been reported adequate to satisfactorily capture the salient responses of structures. Furthermore, the corresponding mathematical simplicity inherent to simple pulse definitions makes them attractive for practical applications. This is consistent with the observation (by Kalkan and Kunnath [8]) that, although simple pulses may not fully capture the characteristic of original earthquakes, the more sophisticated methods of representing or extracting near-fault pulses using wavelets analysis may face some of the same limitations.

The work presented below describes the procedures followed to identify dominant pulses in ground motions, to represent them by equivalent full-sine pulses (consistent with those used in Shrestha and Bruneau [1]), and to predict number of simultaneously yielding stories in a shear-building subjected to earthquake ground motions. These predictions are then compared against results from non-linear analysis. Note that for the study conducted here, simple shear buildings have been considered as opposed to complete designs that may benefit from overstrength introduced by the design process (and that may not have "ideal" shear behavior). Nonetheless, the work presented here is a fundamental step in studying the relationship between story yielding in the building and the velocity waves traveling along the building height, such as to develop a procedure to estimate the number of simultaneously yielding stories due to an earthquake excitation.

2. Analysis parameters

2.1. Structure considered

The same elastic and inelastic systems with uniform and varying story stiffness, defined as Structures-I, -II, -III, and -IV in Shrestha and Bruneau [1], have been considered here. The structures have two percent viscous damping and variation of story yield capacity, V_p, based on the lateral force distribution prescribed by code procedures. The V_p value at the base is made equal to the maximum elastic force demand observed during the entire earthquake history for the case defined as response reduction factor R of 1.0. The V_p values at other stories were then calibrated with respect to the value at the base using the distribution of the V_p values over the building height. Note that the R values will not necessarily be 1 at the other stories. The corresponding four types of structural system are considered as illustrated in Table 1. A response reduction factor R of 4 is considered for the base story. The OpenSees analysis software was used for the dynamic analysis of the structures considered. The model characteristics and nonlinear material properties used for the computer analyses were identical to those described in Shrestha and Bruneau [1].

2.2. Input excitation

The input earthquake excitations considered for the study have been categorized into three groups, depending on the pulse-like characteristic of their velocity record: (i) earthquake excitations having a single dominant pulse in their velocity record, (ii) earthquake excitations having multiple distinct pulses in their velocity record, and; (iii) earthquake excitations that do not have distinct pulses in their velocity record (i.e., non-pulse type earthquake velocity excitation). The three groups of earthquakes considered here, have been referred to as Category A, B, and C respectively. Earthquakes belonging to Categories A and B considered here represent pulse type earthquakes that occur near fault and are known to have more damaging effect on the structure. Six earthquake excitations have been considered in each group, resulting in the eighteen earthquakes listed in Table 2. The velocity time history for these earthquake records are shown in Fig. 1. Some of the earthquake records that have been considered include pulses that have large duration such that the wavelength of the pulse is longer than the height of the building. In such cases, the reflected wave may interfere with the incident wave even before the peak of the velocity wave enters the building. The span of the building over which

Table 1
Structural systems considered.

Case	Structure type				Story stiffness		Response		Damping	V_p variation over height
	I	II	III	IV	Constant over height	Varying over height	Elastic	Inelastic	2%	Code based
1	×				×		×		×	×
2		×			×			×	×	×
3			×			×	×		×	×
4				×		×		×	×	×

Table 2
Earthquake ground motions considered.

Category	No.	Earthquake	ID	Station	Mw	PGA (g)	PGV (cm/s)	PGD (cm)
A	1	1994 Northridge	WPI046	Newhall-W.Pico Canyon Rd.	6.7	0.455	92.8	56.64
	2	1992 Landers	LCN275	Lucerne	7.3	0.785	31.9	16.42
	3	1979 Imperial Valley	H-E04230	El Centro Array #4	6.5	0.36	76.6	59.02
	4	1987 Superstition Hills (B)	B-PTS225	5051 Parachute Test Site	6.7	0.455	112	52.8
	5	1999 Chi Chi, Taiwan	TCU068-N	TCU068	7.6	0.462	263.1	430
	6	1999 ChiChi, Taiwan	CHY101-N	CHY101	7.6	0.44	115	68.75
B	7	1999 Duzce, Turkey	DZC270	Duzce	7.1	0.535	83.5	51.59
	8	1999 Kocaili, Turkey	YPT060	Yarimca	7.4	0.349	62.1	50.97
	9	1994 Northridge	CNP196	Canoga Park-Topanga Canyon	6.7	0.42	60.8	20.17
	10	1989 Loma Prieta	HAD255	1656 Hollister Diff. Array	6.9	0.279	35.6	13.05
	11	1994 Northridge	RO3090	90006 Sun Valley-Roscoe Blvd	6.7	0.443	38.2	10.04
	12	1984 Morgan Hill	CYC285	57217 Coyote Lake Dam (SW Abut)	6.2	1.298	80.8	9.63
C	13	1966 Parkfield	C12320	1016 Cholame #12	6.1	0.063	6.8	3.55
	14	1952 Kern County	HOL090	135 LA Hollywood Stor FF	7.4	0.044	6	2.77
	15	1957 San Francisco	GGP100	1117 Golden Gate Park	5.3	0.112	4.6	0.43
	16	1971 San Fernando	ORR021	24278 Castaic - Old Ridge Route	6.6	0.324	15.6	2.31
	17	1940 Imperial Valley	I-ELC180	117 El Centro Array #9	7	0.313	29.8	13.32
	18	1949 Western Washington State	49OLY	Olympia Test Laboratory	6.5	0.206	16	4.19

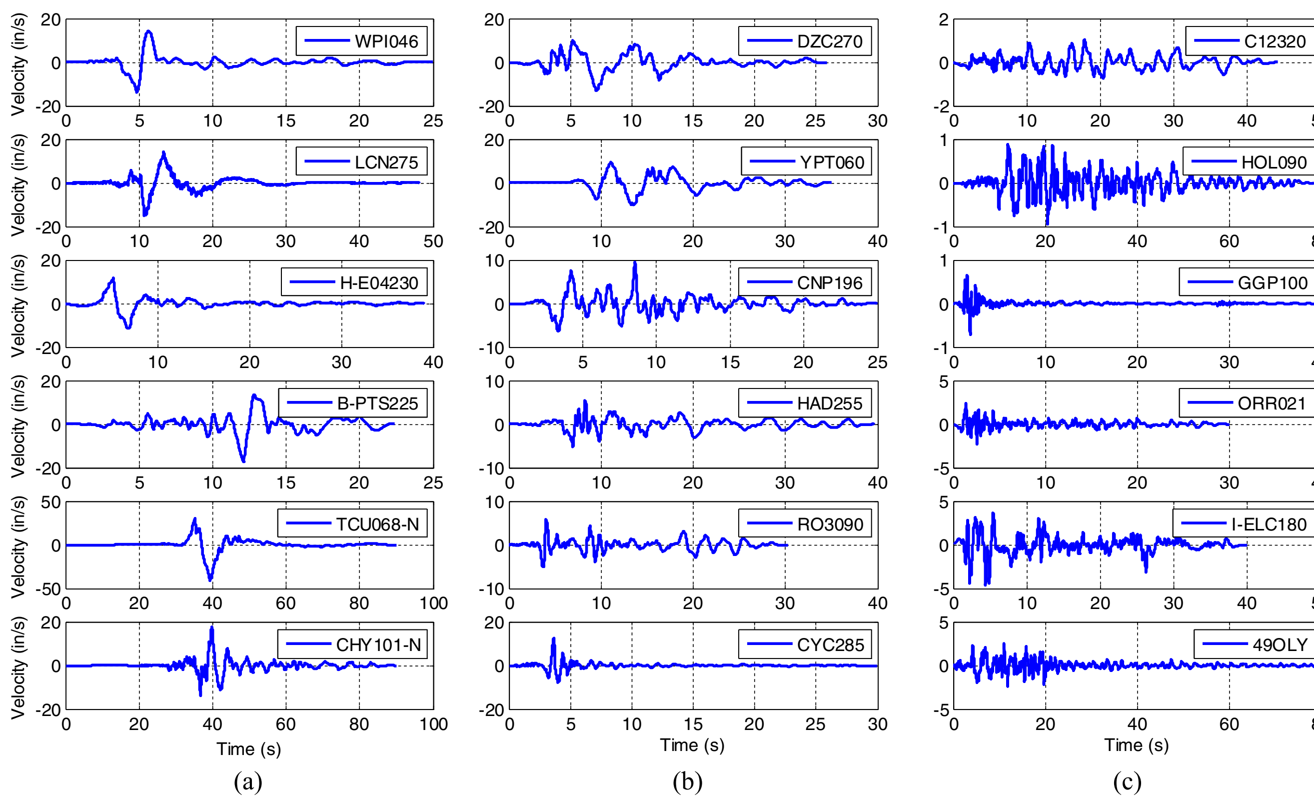

Fig. 1. Earthquake velocity records for original time scale: (a) Category A, (b) Category B, and (c) Category C.

the first half of a pulse extends can be measured by the $t_d/2t_H$ ratio. Here, t_d is the duration of the pulse and t_H is the time take by the wave to travel through the building height H. If $t_d/2t_H$ is greater than 1, the first half of the pulse extends beyond the height of the building and if it is less than 1 the first half of the pulse spans over only some of the stories. Table 3 shows the t_d, $t_d/2t_H$, and t_d/T_n values of the main pulse for the velocity earthquake records considered in the study. For most of the original earthquakes considered here, the $t_d/2t_H$ value for the main pulse is greater than 1 as shown in the table. In order to study the isolated behavior of the incident wave as it travels up the building height, a new set of ground motions, in addition to the original earthquake records, has been considered by condensing the time scale of the acceleration record of the original earthquakes such that the first half of the main pulse covers about half the height of the building. This results in values of $t_d/2t_H$ of around 0.5 and 0.4 for Structure-II and -IV, respectively, and values of t_d/T_n of around 0.25 for both of these structures as shown in Table 3. Note that, as one exception, the time scale of 1957 San Francisco earthquake (GGP100), which already had a short duration pulse, actually was expanded, in an attempt to get a $t_d/2t_H$ of around 0.5 for the structure in that particular case. Alternately, in order to study how the $t_d/2t_H$ ratio affects the story yielding in a building, the height of the building can be changed while keeping the pulse duration constant.

Table 3
The t_d, $t_d/2t_H$, and t_d/T_n values for the earthquake ground motions considered.

EQ #	Earthquake	Original time scale				Condensed time scale			
		t_d (s)	$t_d/2t_H$		t_d/T_n	t_d (s)	$t_d/2t_H$		t_d/T_n
			Str-I	Str-III			Str-I	Str-III	
1	1994 Northridge, Newhall-W.Pico Canyon Rd. (WPI046)	2.53	1.56	1.22	0.77	0.81	0.50	0.39	0.25
2	1992 Landers, Lucerne (LCN275)	4.59	2.82	2.20	1.39	0.81	0.50	0.39	0.25
3	1979 Imperial Valley, El Centro Array #4 (H-E04230)	4.35	2.68	2.09	1.32	0.81	0.50	0.39	0.25
4	1987 Superstition Hills, ParachuteTest Site (B-PTS225)	2.23	1.37	1.07	0.68	0.81	0.50	0.39	0.25
5	1999 Chi Chi, TCU068-N (TCU068-N)	10.93	6.73	5.25	3.32	0.81	0.50	0.39	0.25
6	1999 Chi Chi, CHY101(CHY101-N)	5.54	3.41	2.66	1.68	0.81	0.50	0.39	0.25
7	1999 Duzce, Ducze (DZC270)	4.10	2.52	1.97	1.24	0.81	0.50	0.39	0.25
8	1999 Kocaili, Yarimca (YPT060)	3.53	2.17	1.70	1.07	0.81	0.50	0.39	0.25
9	1994 Northridge, Canoga Park-Topanga Canyon (CNP196)	2.08	1.28	1.00	0.63	0.81	0.50	0.39	0.25
10	1989 Loma Prieta, Hollister Diff. Array (HAD255)	2.66	1.64	1.28	0.81	0.81	0.50	0.39	0.25
11	1994 Northridge, Sun Valley-Roscoe Blvd (RO3090)	1.06	0.65	0.51	0.32	0.81	0.50	0.39	0.25
12	1984 Morgan Hill, Coyote Lake Dam (SW Abut) (CYC285)	1.01	0.62	0.49	0.31	0.81	0.50	0.39	0.25
13	1966 Parkfield, Cholame#12 (C12320)	3.32	2.04	1.60	1.01	0.81	0.50	0.39	0.25
14	1952 Kern County, LA Hollywood Stor FF(HOL090)	2.92	1.80	1.40	0.89	0.81	0.50	0.39	0.25
15	1957 San Francisco, Golden Gate Park (GGP100)	0.46	0.28	0.22	0.14	0.81	0.50	0.39	0.25
16	1971 San Fernando, Castaic - Old Ridge Route (ORR021)	0.97	0.60	0.47	0.30	0.81	0.50	0.39	0.25
17	1940 Imperial Valley, El Centro Array #9 (I-ELC180)	2.47	1.52	1.19	0.75	0.81	0.50	0.39	0.25
18	1949 Western Washington State, Olympia Test Laboratory (49Oly)	2.00	1.23	0.96	0.61	0.81	0.50	0.39	0.25

3. Main pulse of an earthquake excitation

An earthquake excitation can be considered to consist of a series of pulses with varying amplitude and frequency. When a building is excited by an earthquake input, this series of pulse enters the buildings, and some of those pulses will cause stories to yield. Story forces and hence story yielding was found to be related to the velocity waves propagating along the building height (Shrestha and Bruneau [1]). This is consistent with observations by Krishnan and Muto [9] who reported that structural response is "extremely sensitive to the peak ground velocity". Here, upon reviewing the story yield patterns in the case study building subjected to various earthquake excitations, it was observed that the biggest pulse in the earthquake velocity record was typically responsible for causing the maximum number of stories to yield simultaneously, as seen in Figs. 2 to 4, for some of the representative earthquakes belonging to the three categories described above. This suggested that if this pulse, referred to as the main/dominant pulse here, could be identified, the maximum number of simultaneously yielding stories required for calculating the axial force demand in columns could be estimated.

3.1. Identifying the main pulse of an earthquake velocity record

To identify the main pulse in an earthquake velocity record that has the likelihood of causing the maximum number of stories to yield simultaneously, the amplitude and width of the pulse should be given due consideration. The amplitude of the velocity pulse determines the capability of an earthquake to cause yielding at different stories in the building. Shrestha and Bruneau [1] noted that story yielding will occur if the value of the $\Delta u/t_h$ wave (i.e., $-v_f+v_b$) at that story is greater than its v_y value, where, Δu is the inter-story drift, t_h is the time taken by the wave to travel through the story

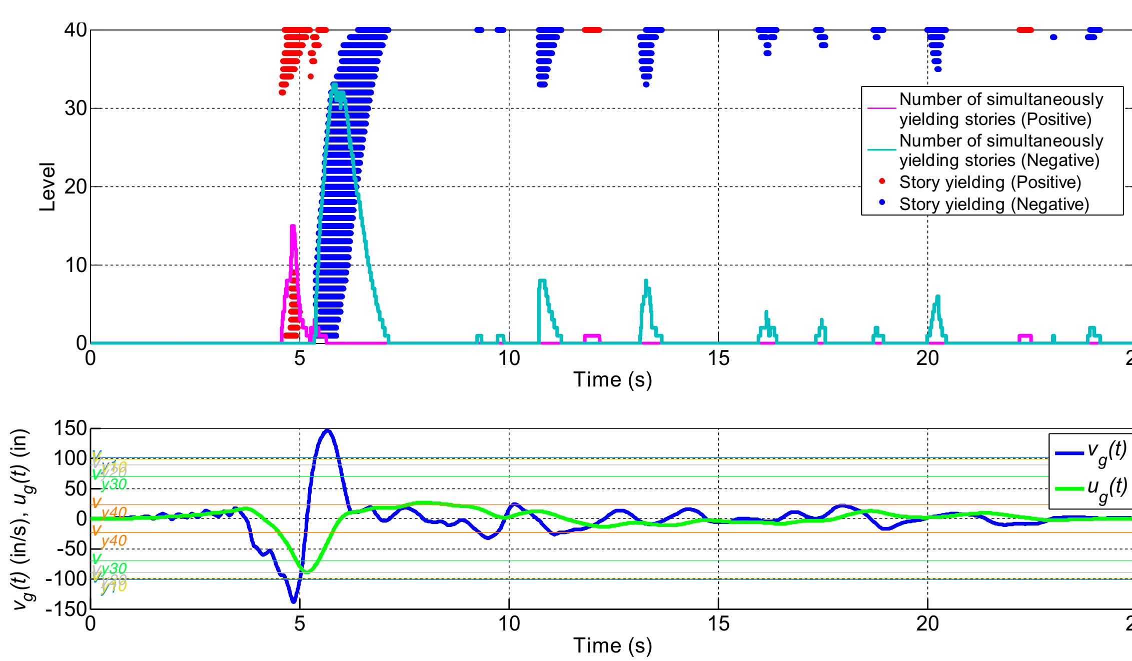

Fig. 2. Story yield pattern for Structure-IV subjected to 1994 Northridge (WPI046) earthquake record with original time scale.

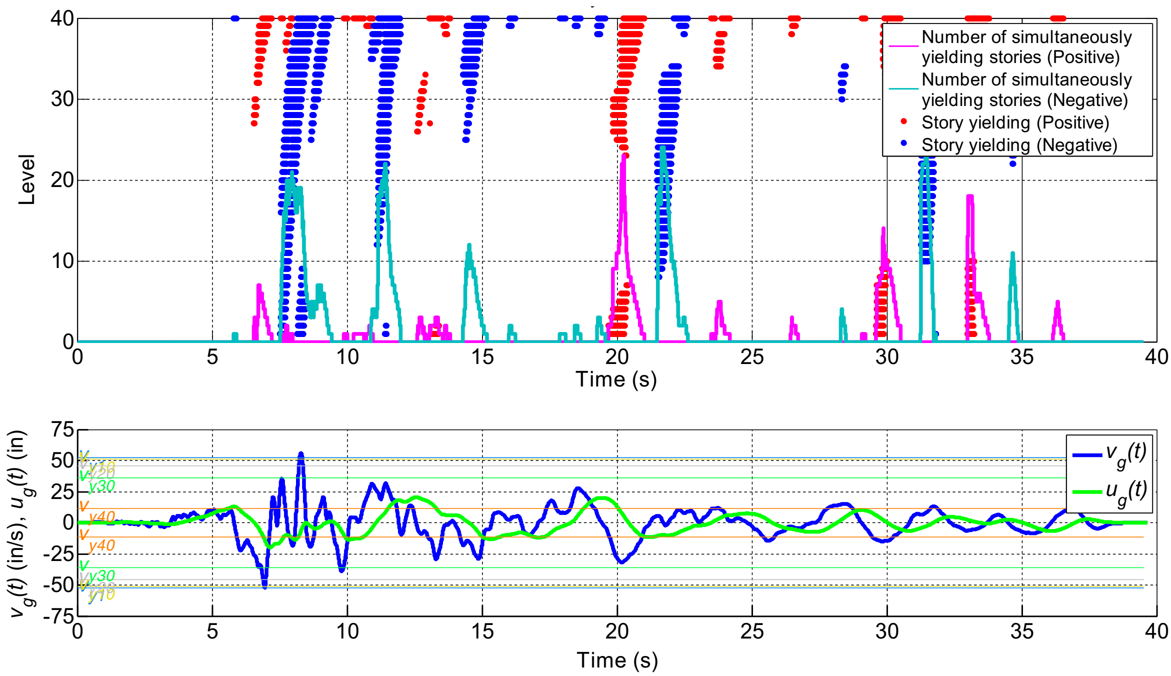

Fig. 3. Story yield pattern for Structure-IV subjected to 1989 Loma Prieta, Hollister Diff. Array (HAD255) with original time scale.

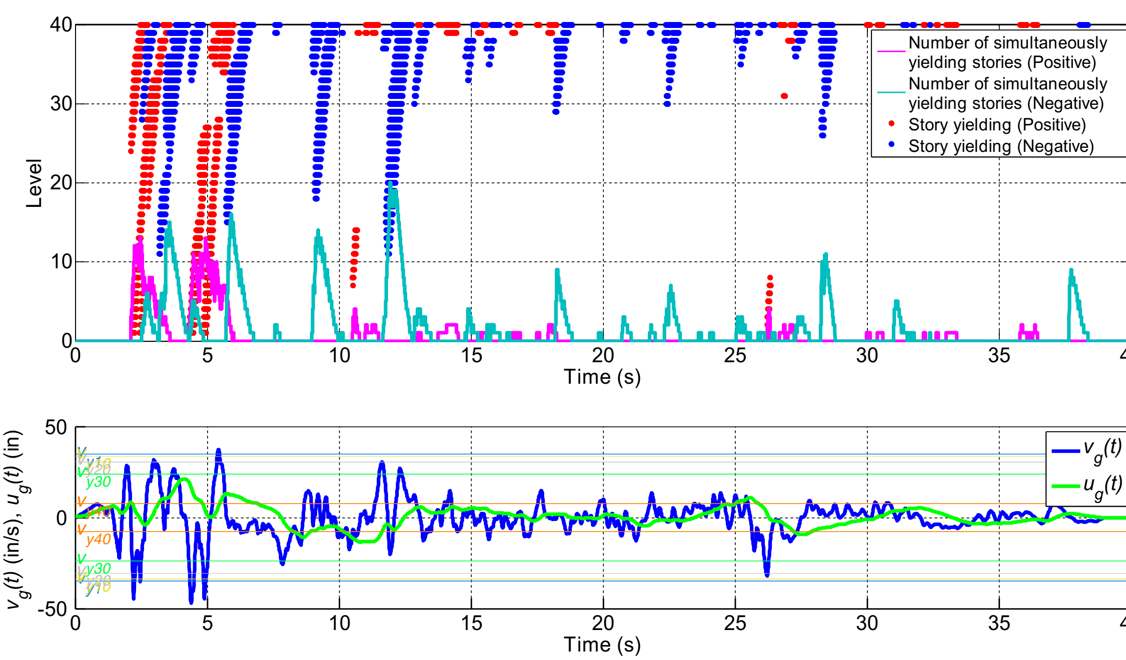

Fig. 4. Story yield pattern for Structure-IV subjected to 1940 Imperial Valley, El Centro Array #9 (I-ELC180) earthquake record with original time scale.

with height h, v_f is the forward moving velocity wave, and v_b is the backward moving velocity wave. Combined to the above, the duration of the velocity pulse gives a measure of the number of stories that can yield simultaneously. Keeping these two considerations in mind, the main/dominant pulse in the earthquake records considered was identified using two different approaches: (i) based on a visual review of the ground velocity record and using judgment, and (ii) by following more rigorous step-by-step procedure (which was used to develop a computer program to identify the main pulse).

3.1.1. Judgmental method

In the judgmental method, the main pulse of the velocity earthquake record is identified by visual inspection of the series of pulses contained in the record. The magnitude of the pulses are compared against the v_y values of the stories and the number of stories the candidate pulses can likely yield are compared. For the pulse dominant earthquakes in the first group of earthquakes considered, it is relatively straight-forward to distinguish the dominant pulse. For the other two earthquake categories considered, choosing the dominant pulse requires more judgment.

For the second type of earthquake, which may have more than one distinct pulse, the pulse having $v_g(t)$ values greater than v_y values for a large number of stories and a width that can simultaneously yield the maximum number of stories should be considered. For example, in ground motion record CNP196 (Fig. 5a), pulses A and B both have amplitude greater than the v_y values of most stories in the building; thus, both have the ability to cause yielding in those stories. However, pulse A is wider than pulse B, and can therefore cause a larger number of stories to yield simultaneously than pulse B. Thus, pulse A is identified as the dominant pulse.

For another example, in the RO3090 earthquake record (Fig. 5b), pulse A has an amplitude greater than the v_y values at all the stories, while the amplitude of pulse B is greater than v_y values only

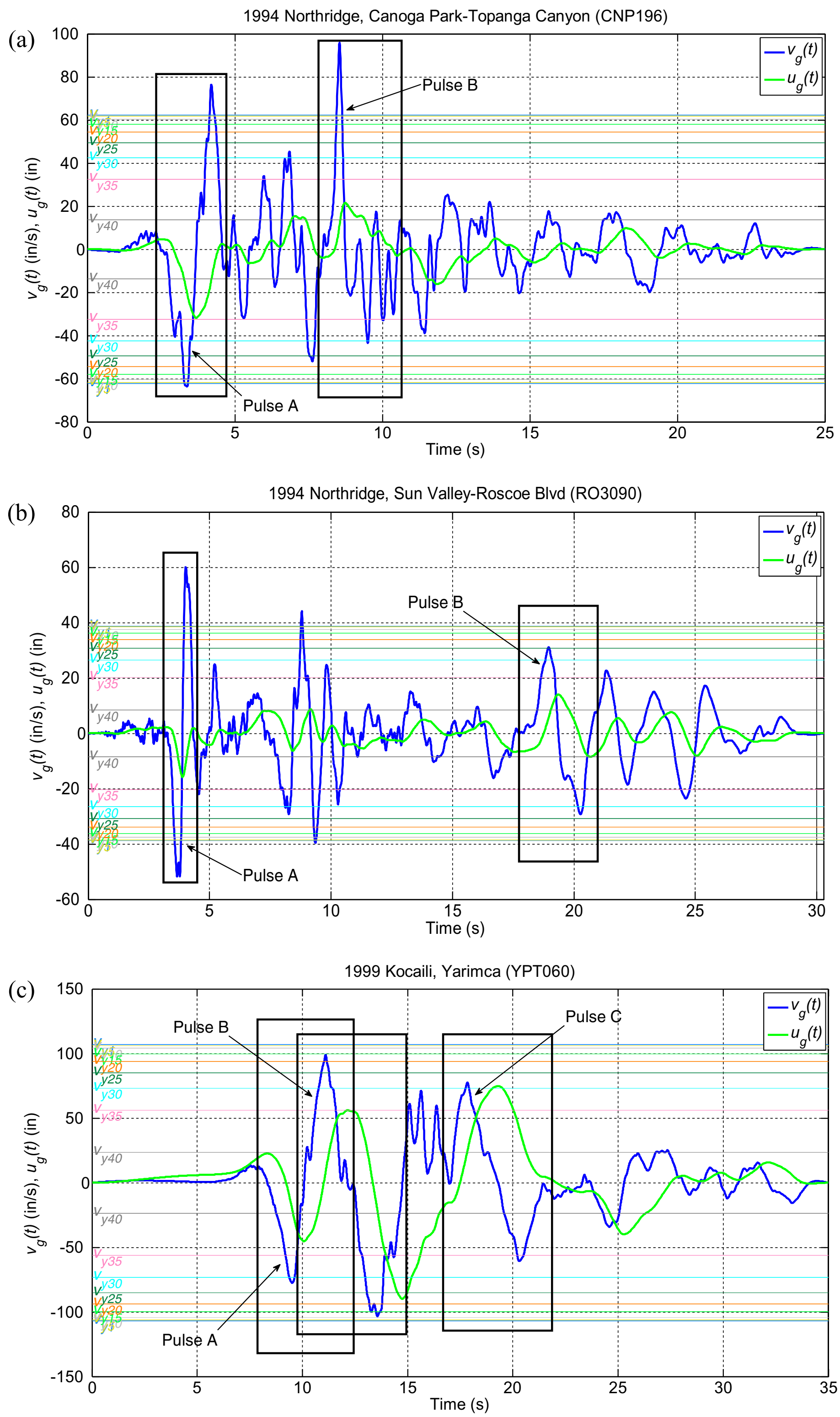

Fig. 5. Examples of earthquake records having multiple distinct pulses (Category B).

over stories 22 to 40. However, the duration of pulse B is comparatively longer than the duration of pulse A, and it can cause a larger number of stories to yield simultaneously. Thus, in this case, pulse B can be the dominant pulse.

Note that while the above proved to work in most cases, it cannot be predicted to be the case with an absolute certainty. There is always the possibility that a smaller pulse of opposite sign occurring just before the candidate dominant pulse can affect its story yielding capacity, as it deforms the structure in the opposite direction prior to the "hit" of the potentially dominant pulse. Thus, if there is more than one potentially dominant pulse, the pulse with the smaller preceding pulse should be chosen. For example, in ground motion YPT060 (Fig. 5c), pulse B has the largest amplitude and the longest duration compared to all other pulses in the earthquake record. But there is a smaller pulse preceding it, which can significantly affect the story yielding capacity of pulse B. Thus, instead of pulse B, pulse A should be considered as the dominant pulse. Though the first part of pulse A has lower amplitude than the v_y values of the stories up to around 18 stories, it can still cause a larger number of stories to yield compared to pulse B.

The third type of earthquake category considered is the non-pulse type earthquake that does not have distinct pulses. In such case, it is challenging to identify a dominant pulse. Yet, the technique presented in the preceding paragraph can be applied as well. However, because earthquakes in this category usually tend to have many successive and comparable pulses, there are more chances that a candidate pulse may be affected by the preceding pulses. Choosing the dominant pulse from the pulses towards the beginning of the record, as well as considering pulses that are least affected by previous pulses, has generally provided good results. Note that, in some cases, there may be series of short duration one sided pulses. If such pulses are close to each other, they can be lumped into one single big pulse. For example, in earthquake record I-ELC180 (Fig. 6), pulse A has two dominantly one sided pulses. These two pulses can be combined into one single pulse. Doing so may give conservative result but helps in simplifying the procedure.

3.1.2. Systematic procedure

Based on the same concepts as described for the judgmental method, in the systematic procedure, the main pulse of the velocity earthquake record is identified by following more rigorous and systematic steps. The following steps can be followed to formulate a systematic procedure to identify the main pulse in an earthquake record (for more detailed descriptions refer to Shrestha and Bruneau [10]):

1. Plot the displacement and velocity input ground excitation using a common axis. Also draw horizontal lines corresponding to the v_y values at different stories in the building, as shown for example in Fig. 7a. for the case of 1994 Northridge, Canoga Park-Topanga Canyon (CNP196) earthquake. The v_y values shown are for Structure-IV with V_p variation based on code specified lateral force distribution.
2. Locate the peaks/troughs along the displacement curve and find their amplitudes.
3. Determine the number of candidate velocity pulse, N_C.
4. Identify the first N_C peaks/troughs that have the largest amplitudes. Also identify the displacement pulse, similar in shape to the displacement pulse of a full-sine velocity pulse, corresponding to these peaks/troughs. Fig. 7b shows the three largest peaks/troughs and the beginning and end of the respective displacement pulses.
5. Identify the candidates for the main velocity pulse and use the following approach to fit an equivalent full-sine velocity pulse: (a) Set the point at which the displacement pulse attains its maximum value to correspond to the midpoint of the velocity pulse that has zero value; (b) Set the starting point of the candidate velocity pulse at the point with zero velocity that lies before the start of the corresponding displacement curve, and; (c) Set the end point of the velocity pulse at the point along the velocity curve that has zero magnitude and lies after the end of the corresponding displacement pulse. For example, the beginning and end of the three candidate pulses A, B, and C for the 1994 Northridge, Canoga Park-Topanga Canyon (CNP196) earthquake are shown in Fig. 7b.
6. Find the value of the "nw_{avg}" product for each candidate pulse. Here, n is the number of stories that have their v_y values lower than the amplitude of the first part of the pulse, and w_{avg} is the average width of first part of the candidate velocity pulse below the highest v_y value or the peak of the candidate velocity pulse, whichever is larger. In the example shown in Fig. 7b, the amplitude of pulse C is larger than the v_y values of stories above the 35th story, so it can yield stories above 35th stories only. However, amplitudes of pulses A and B are larger than the v_y values at all the stories; thus, both pulses can yield all the stories. But, since the width of pulse A is wider than that of pulse B, pulse A will have the largest nw_{avg} value and can cause a larger number

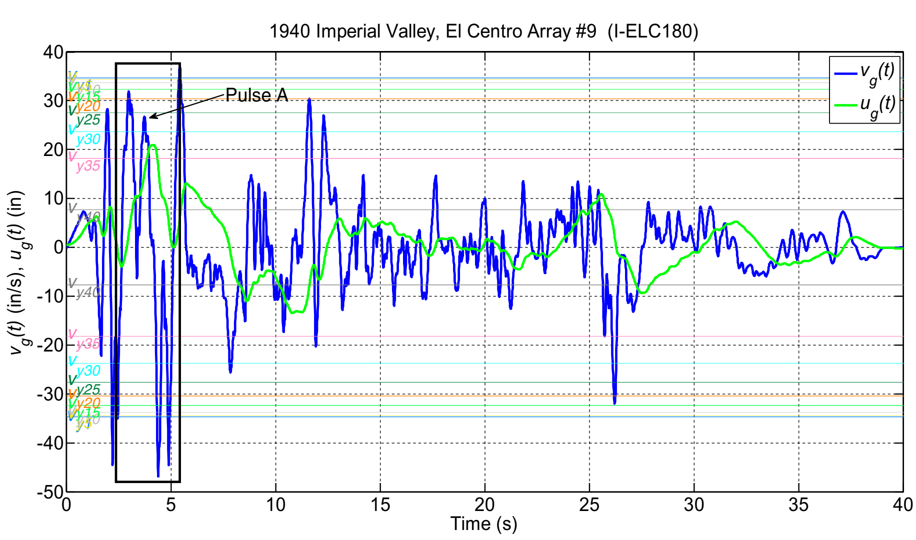

Fig. 6. Example of non-pulse type earthquake record having series of one sided pulse (Category C).

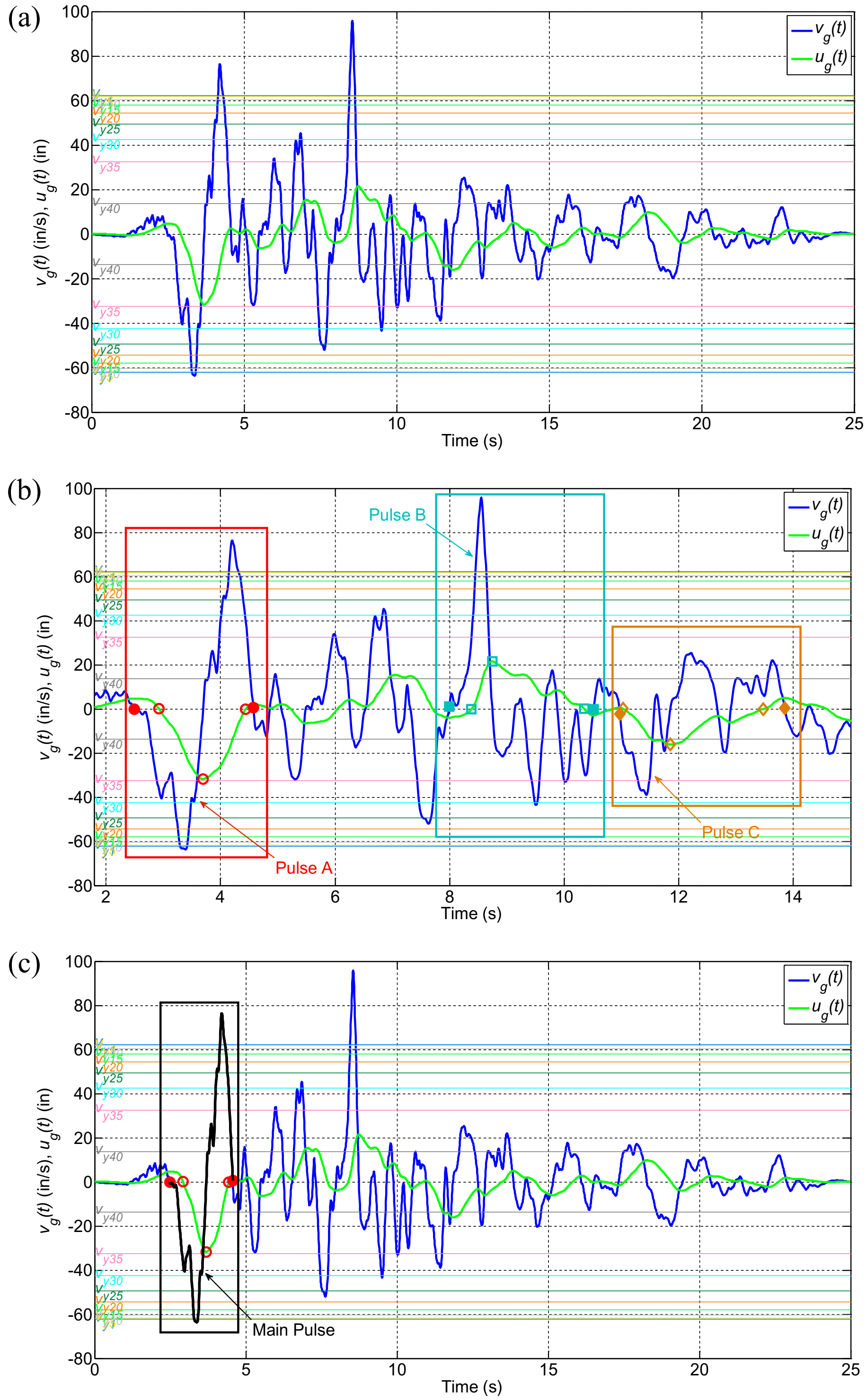

Fig. 7. Identification of main pulse using systematic procedure for 1994 Northridge, Canoga Park-Topanga Canyon (CNP 196) (a) displacement and velocity record, (b) candidate pulses, and (c) main pulse.

of stories to yield simultaneously. Thus, pulse A (Fig. 7c) is the most likely dominant pulse, based on the nw_{avg} value of the candidate pulse (provided there is no preceding pulse).

7. If there is a preceding pulse that pushes the building in the opposite direction of the candidate pulse, then the preceding pulse can decrease the yielding capacity of the candidate pulse. In such case, find the nw_{avg} value for the preceding pulse of the candidate pulses and then find the ratio of nw_{avg} values of the preceding pulse to that of the respective candidate pulse (i.e. find $nw_{avg,preceeding}/nw_{avg,candidate}$).
8. Optionally, eliminate the candidate velocity pulses that have a large value of this ratio; for example if a candidate pulse has $nw_{avg,preceeding}/nw_{avg,candidate}$>0.5 (say), it should be eliminated, as it will be considerably affected by its preceding pulse.

9. After this elimination process, chose the velocity pulse from the remaining candidate pulses that has the largest $nw_{avg,candidate}$ value. This pulse will be the dominant velocity pulse in the earthquake record. In the example above, pulses A, B, and C all are preceded by pulses acting in the opposite direction. Comparing the size of the pulses, Pulse A has the largest area relative to its preceding pulse; thus, it will be least affected by the preceding pulse. Therefore, based on this, pulse A is retained as the most likely dominant/main pulse.

A flow-chart of the above procedure is provided in Fig. 8. Based on steps illustrated above, a computer program can be generated to make identification of the main pulse much easier. One such computer program was developed by the authors and is presented in Shrestha and Bruneau [10]. It was used to identify the main pulse using the systematic procedure for the research presented here. The program was found to work efficiently as can be seen in Section 3.1.3

3.1.3. Comparison of results from judgmental and systematic procedures

Fig. 9 shows the resulting dominant pulse, obtained using the judgmental approach for identifying the main pulse for some of the representative earthquakes with original time scale belonging to the three categories. For these earthquakes, the Matlab code developed for identification of the main pulse of the velocity record yielded the same main pulse as obtained by the judgmental method. Note that the dominant pulse identified by the two methods matched for most of the earthquakes, except for 4 out of 18 earthquakes considered (namely, the 1966 Parkfield, 1957 San Francisco, 1971 San Fernando, and 1949 Western Washington State records, belonging to category C which are non-pulse type earthquakes) for the case of earthquakes with original time scale. For the case of earthquakes with condensed time scale, in addition to the above four earthquakes, the dominant pulse identified by the two methods also differed for 1940 Imperial Valley belonging to category C and 1989 Loma Prieta belonging to category B (earthquake with more than one distinct pulse). The main pulse identified using the judgmental approach was found to give slightly better results for the main pulse of the earthquakes considered. Therefore, the main pulse identified using the judgmental approach were the ones used in the research work. Note that even though the main pulse identified by the two methods may be different, the N_{SYS} values predicted by the two results would not differ significantly. The computer program written for identifying the main pulse using the systematic method was considered to work effectively. The objective of generating the computer program was mainly to simplify the procedure by automation.

3.2. Idealizing the main pulse

Since the main pulse in the velocity record is responsible for causing the maximum number of stories yielding simultaneously, this main pulse was isolated from the original earthquake record and idealized by an equivalent full-sine velocity pulse. Here, a simple method was adopted to idealize the velocity pulse. The time period of the idealized pulse was chosen to be equal to the time period of the isolated main pulse, and amplitude of the idealized pulse was made equal to the average value of the positive and negative amplitude of the isolated pulse. Given that the first part of the wave is the one that typically determines the number of stories yielding simultaneously, the amplitude and time period of the idealized pulse could have also been defined based solely on the first part of the velocity pulse. However, here equal weight was given for both the positive and the negative amplitude of the velocity pulse. Although this idealization was believed to be simple and expected to give conservative results for long duration pulse that are not symmetric in shape, it was found to adequately capture the width and amplitude of the main pulse of the velocity record. Fig. 10 shows the idealized dominant pulse of the velocity record

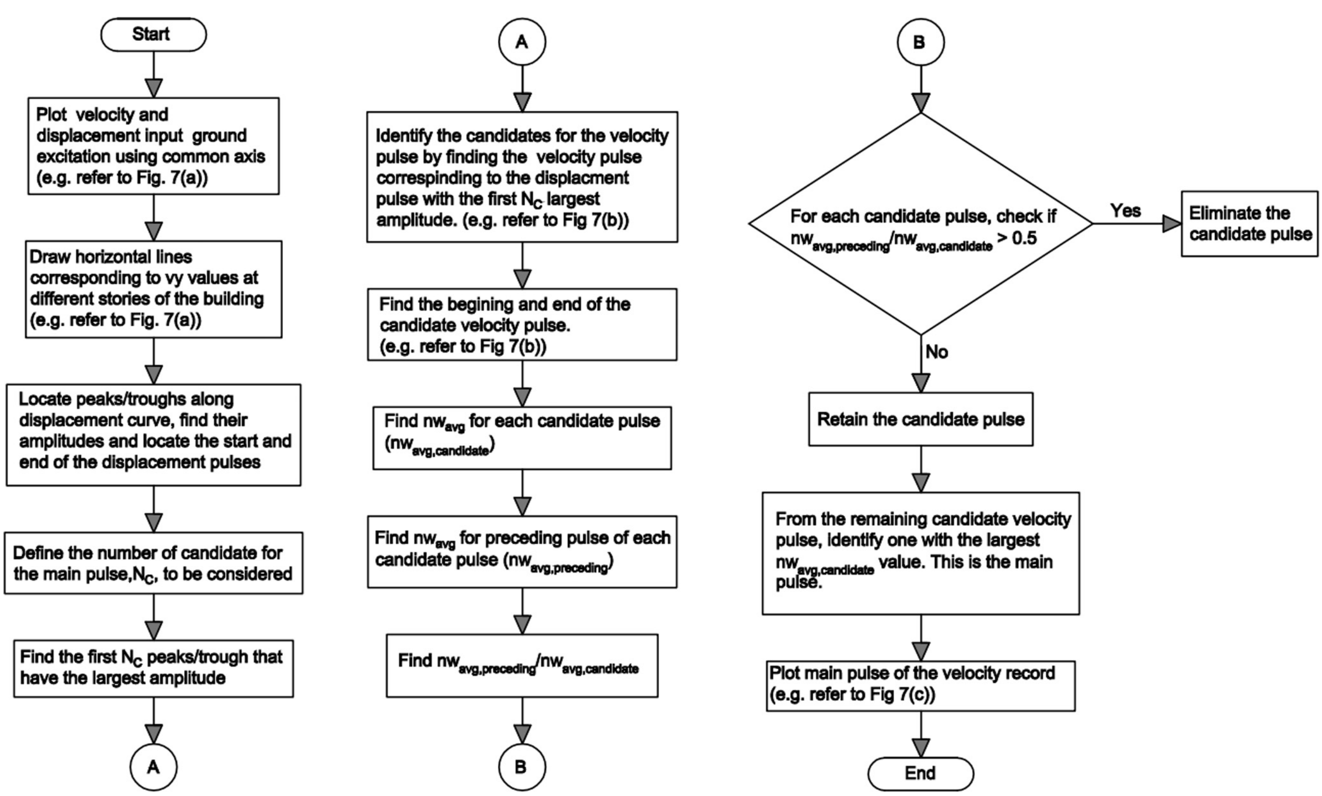

Fig. 8. Flowchart to identify the main pulse of an earthquake velocity record using systematic procedure.

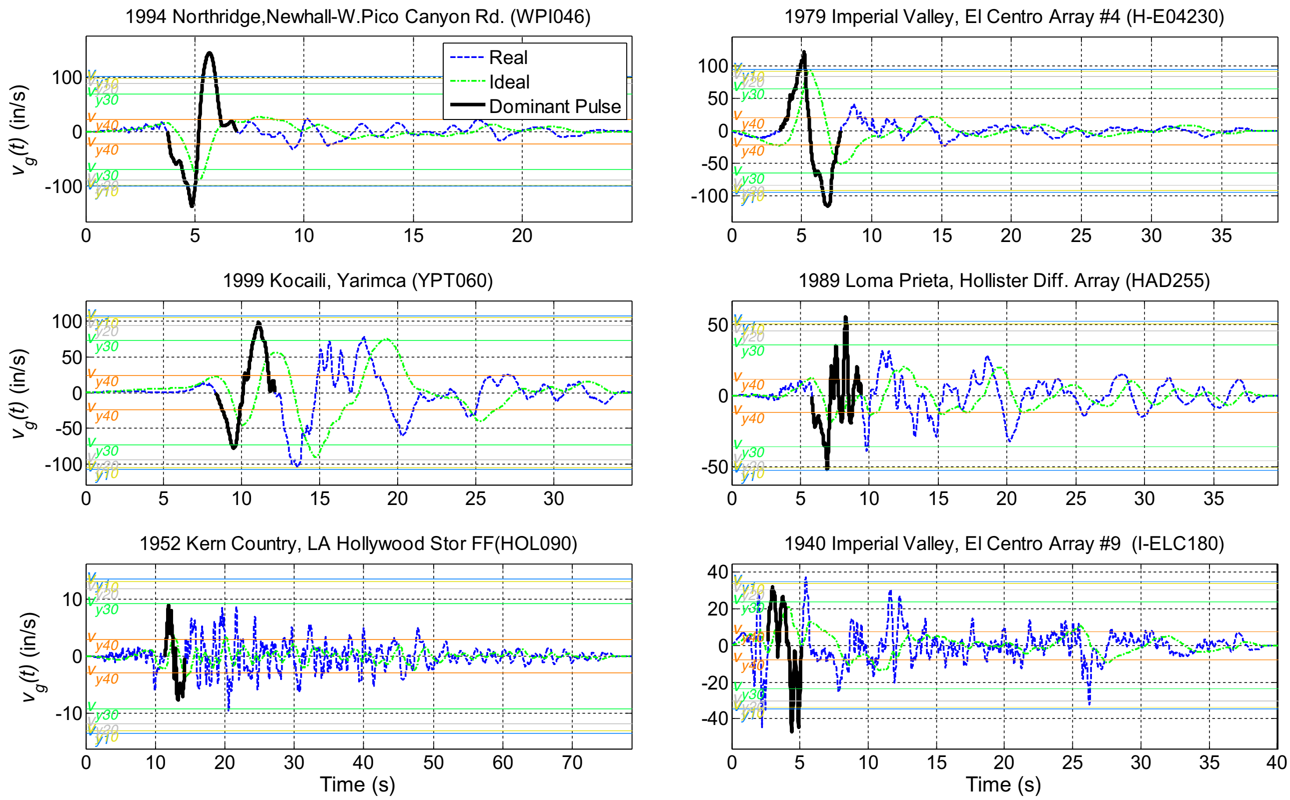

Fig. 9. Dominant pulse in velocity records of some of the representative earthquakes (with original time scale) belonging to the three categories of earthquakes, obtained by judgmental approach.

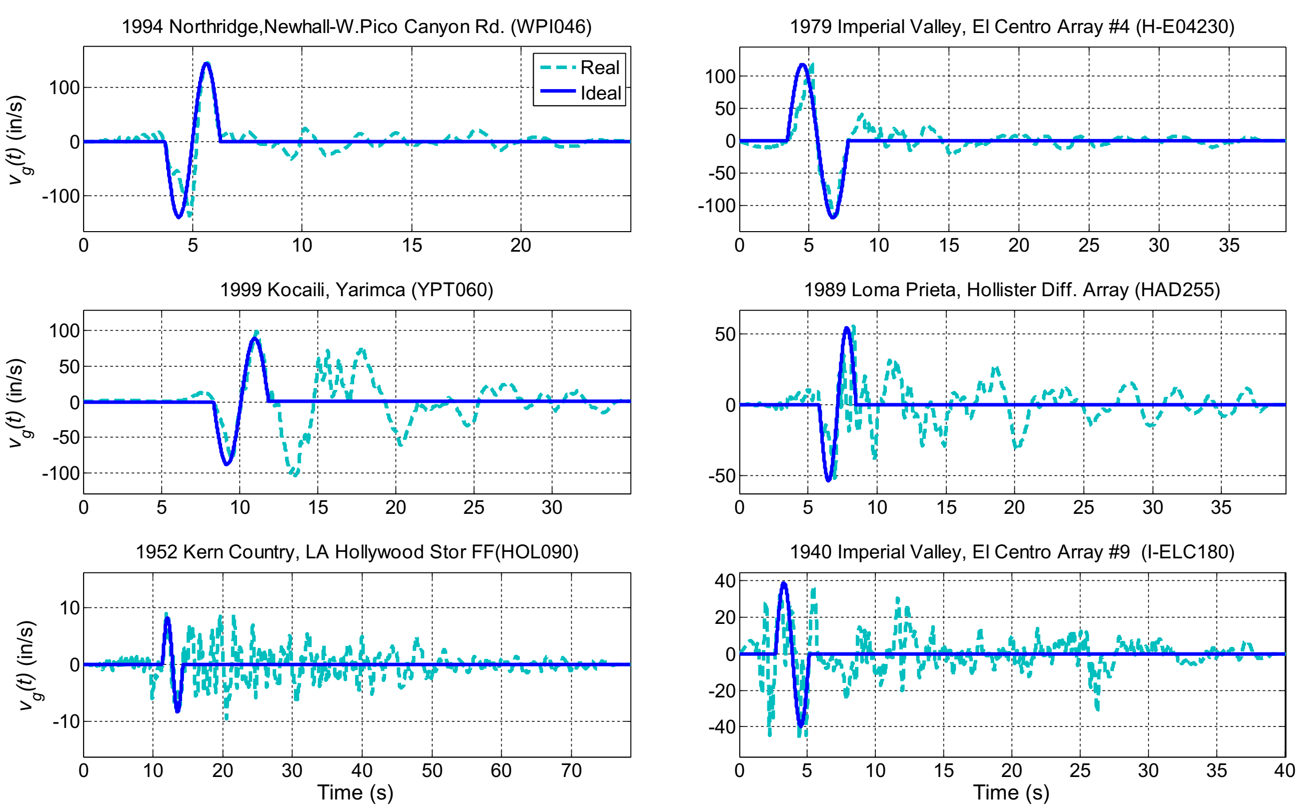

Fig. 10. Idealized dominant pulse of some of the representative earthquakes (with original time scale) belonging to the three categories of earthquakes.

for the earthquakes with original time scale for some of the representative earthquakes belonging to the three categories.

4. Number of simultaneously yielding stories

Simultaneous story yielding can occur due to the incident wave, or due to the constructive overlapping of the forward moving velocity wave (with reverse sign) and backward moving velocity wave occurring at the top and base of the building (as described in Shrestha and Bruneau [1]). While calculating the axial force demand in the columns, these three cases of simultaneous story yielding should be considered.

Once the main pulse in the earthquake record is identified and idealized as a full-sine velocity pulse, the number of simultaneously yielding stories can be predicted by using the mathematical formulation presented in Shrestha and Bruneau [1]. Here, the estimations were done using both methods presented there, namely: (i) considering the shape of the main pulse to be a full-sine velocity pulse, and (ii) by assuming the shape of the velocity pulse to be rectangular. The number of simultaneously yielding stories due to the incident wave are denoted by $N_{SYS,Incident}$.

In the first method, the time at which yielding initiates, denoted by t_{Cj}, and ends, denoted by t_{Dj}, at j^{th} story can be calculated using Eqs. (1) and (2) respectively.

$$t_{Cj} = \frac{1}{\omega_d}\sin^{-1}\left(\frac{v_{yj}}{v_{g0}}\right) + \sum_{i=1}^{j} t_{hi} \tag{1}$$

$$t_{Dj} = \frac{t_d}{2} - \frac{1}{\omega_d}\sin^{-1}\left(\frac{v_{yj}}{v_{g0}}\right) + \sum_{i=1}^{j} t_{hi} \tag{2}$$

Here, v_{g0} is the amplitude and w_d is the radial frequency of the full-sine velocity pulse (idealized pulse here) with time period t_d. The time taken by the wave to travel through the j^{th} story with mass $\bar{m}_j$, height h_j, and story stiffness k_j is denoted by t_{hj}; it can be calculated using Eq. (3).

$$t_{hj} = \sqrt{\frac{h_j \bar{m}_j}{k_j}} \tag{3}$$

Once the t_{Cj} and t_{Dj} values at all levels are known, the data can be interpolated to find the topmost and lowermost story yielding simultaneously, denoted by lvl_C and lvl_D respectively, at any time 'T (refer to Shrestha and Bruneau [1] for more detail). The difference between the two will give the number of simultaneously yielding stories at time T as shown in Eq. (4).

$$N_{SYS} = lvl_C - lvl_D \tag{4}$$

In the second method, Eqs. (5) and (6) can be used to find the height of the topmost and lowermost story yielding simultaneously denoted by x_C and x_D respectively, at a given time 'T.

$$x_C = \begin{cases} H\sin\left(\sqrt{\frac{hk_b}{\bar{m}H^2}}T\right) & t_{C,\min} \leqslant T \leqslant t_{C,\max} \\ x_{y,\max} & t_{C,max} \leqslant T \leqslant t_{D,\max} \end{cases} \tag{5}$$

and,

$$x_D = \begin{cases} x_{y,\min} & t_{C,\min} \leqslant T \leqslant t_{D,min} \\ H\sin\left\{\sqrt{\frac{hk_b}{\bar{m}H^2}}\left(T - \frac{t_d}{2}\right)\right\} & t_{D,\min} \leqslant T \leqslant t_{D,\max} \end{cases} \tag{6}$$

Here, h is the story height, H is the building height, k_b is the story stiffness of the base story, $\bar{m}$ is the story mass, $x_{y,\min}$ denotes the lowermost story with v_y value less than the amplitude of the incident velocity wave; while, $t_{C,\min}$ and $t_{D,\min}$ respectively denote the t_{Cj} and t_{Dj} values for that story. Similarly, $x_{y,\max}$ denotes the uppermost story with v_y value less than the amplitude of the incident velocity wave; while, $t_{C,\max}$ and $t_{D,\max}$ respectively denote the t_{Cj} and t_{Dj} values for that story. The number of simultaneously yielding stories N_{SYS} can then be estimated using Eq. (7).

$$N_{SYS}(T) = \frac{x_C - x_D}{h} \tag{7}$$

In order to find the number of simultaneously yielding stories due to the overlapping at the top and bottom of the building, denoted by $N_{SYS,Top}$ and $N_{SYS,Base}$ respectively, for expediency, the rough estimation described below was done, which gives conservative results. In this approach, the v_y values of the stories falling within the region of the overlap are compared against the amplitude of the constructive overlap of the velocity waves (i.e., $2v_{g0}$ value, where v_{g0} is the amplitude of the idealized main pulse of the earthquake velocity record). When the v_y value was less than $2v_{g0}$ values, then that story was considered to yield during the overlap. Thus, the number of stories yielding simultaneously due to the overlap is equal to the number of stories within the span of the overlap that have v_y values less than two times the amplitude of the velocity base excitation. Note that in the case of an inelastic medium, since velocity waves gets deformed due to the yielding in the stories, the overlapping would not be exactly as in the elastic medium, but roughly similar to the elastic case. However, for simplicity, the number of simultaneously yielding stories due to the overlaps is estimated without considering the change in shape of the wave.

5. Results

5.1. Comparison of yield patterns

Figs. 11 to 13 show typical examples for comparison of the yield patterns due to the actual earthquake, isolated main pulse, and idealized main pulse. The story yield patterns due to the main pulse of the actual earthquake and those due to the idealized pulse are reasonably close. The idealized main pulse is found to slightly (and conservatively) overestimate the number of stories yielding due to the incident wave as compared to the actual earthquake in most of the cases (14 out of 18 earthquakes, for both earthquakes with original and condensed time scale), since it generally has a larger width compared to the main pulse of the actual velocity record considered and also because it is not subjected to any "interference" from the preceding pulse. For example, for Structure-IV, the maximum number of stories yielding simultaneously due to the incident wave of the main pulse is 15 during the actual earthquake, while it is 20 due to the idealized main pulse for the 1994 Northridge, Newhall-W.Pico Canyon Rd. (WPI046) with original time scale (Fig. 11). Similarly, for the same structure, the N_{SYS} values due to the incident wave are 7 and 19 for the actual and idealized main pulse, respectively, for the 1989 Loma Prieta, Hollister Diff. Array (HAD255) earthquake record with original time scale (Fig. 12), and 15 and 19 for actual and idealized main pulse, respectively, for the 1940 Imperial Valley, El Centro Array #9 (I-ELC180) with original time scale (Fig. 13). The N_{SYS} values due to the actual and idealized main pulses are closer for earthquakes with condensed time scale in comparison to earthquakes with original time scale. On average, for all the earthquakes considered, the N_{SYS} value due to the idealized pulse is 27% more than that due to the actual main pulse for earthquakes with condensed time scale, while it is 107% more in case of earthquakes with original time scale. Although conservative, it is found to provide reasonably good prediction of the N_{SYS} values.

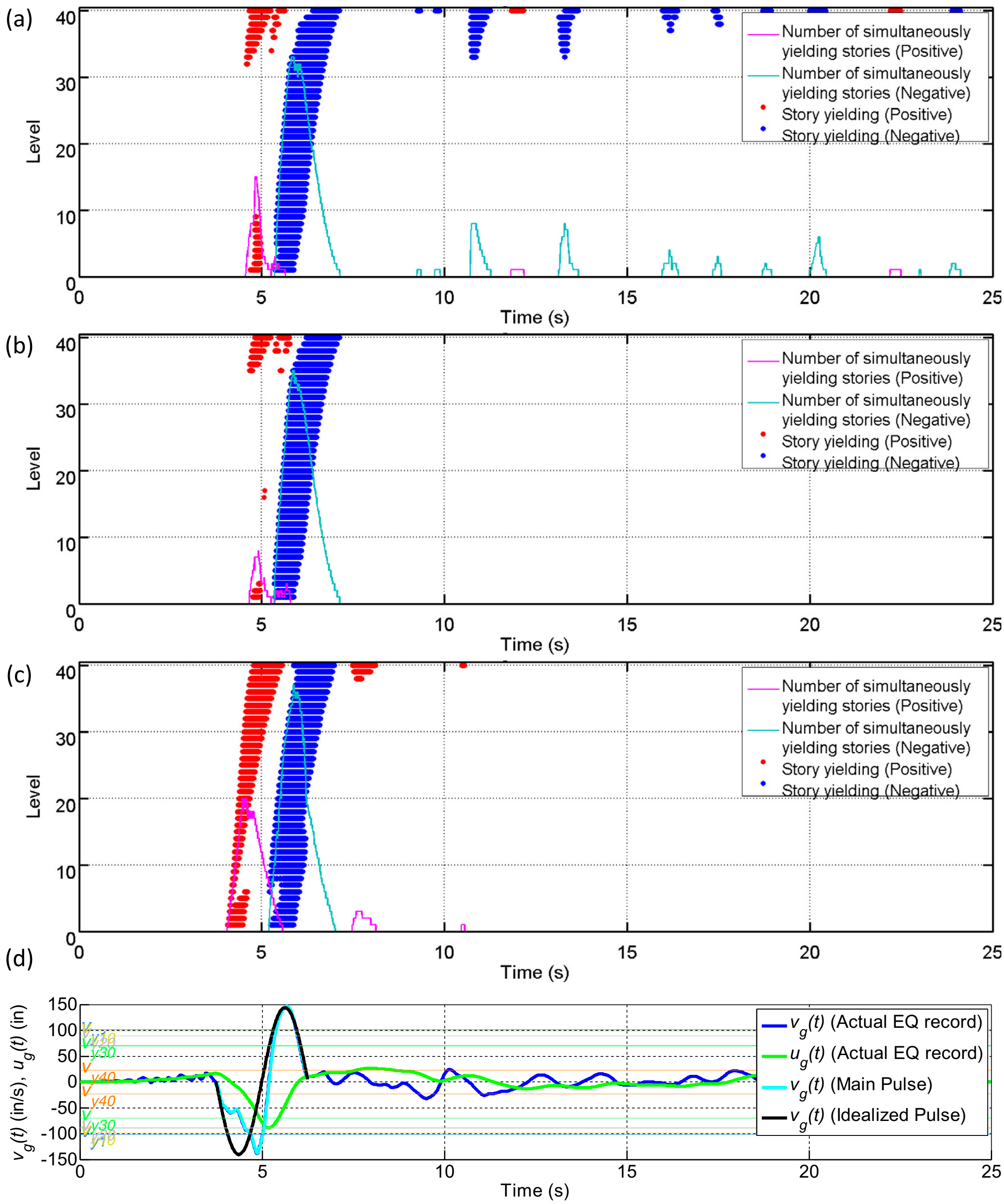

Fig. 11. Story yield time history of Structure-IV subjected to: (a) actual earthquake record, (b) isolated main pulse, and (c) main pulse idealized as full-sine velocity pulse, for 1994 Northridge (Newhall-W.Pico Canyon Rd.) earthquake with original time scale.

5.2. Estimation of N_{SYS} values

Story yield pattern observed due to the actual earthquake record and the t_C and t_D curves that predict the story yielding due to the incident wave of the idealized main pulse are shown in Figs. 14 to 19 for earthquakes with original and condensed time scale. Though both the methods of predicting the N_{SYS} values were used for the estimation, (i.e., (i) considering the shape of the main pulse to be a full-sine velocity pulse, and (ii) by assuming the shape of the velocity pulse to be rectangular), results for the first estimation method only are presented since t_C and t_D obtained considering this method gives better prediction of the story yielding. Note that although analysis for Structure-II was also conducted, only results for Structure-IV (which has story stiffness varying over the building height and is more realistic) are presented here.

Estimated number of simultaneously yielding stories due to the incident wave and due to the overlapping at the top and bottom are shown in Tables 4 and 5 for Structure-IV subjected to earthquakes with original and condensed time scale, respectively. The maximum number of simultaneously yielding stories observed as the incident wave travels to the top of the building is denoted by $MN_{SYS,Incident}$. The estimated maximum number of simultaneously yielding stories (i.e. the maximum of the estimated $MN_{SYS,Incident}$, $N_{SYS,Top}$, and $N_{SYS,Base}$) is obtained and compared to the value obtained from OpenSees analyses (i.e., the actual values obtained from earthquake excitations). Discrepancy between the two values

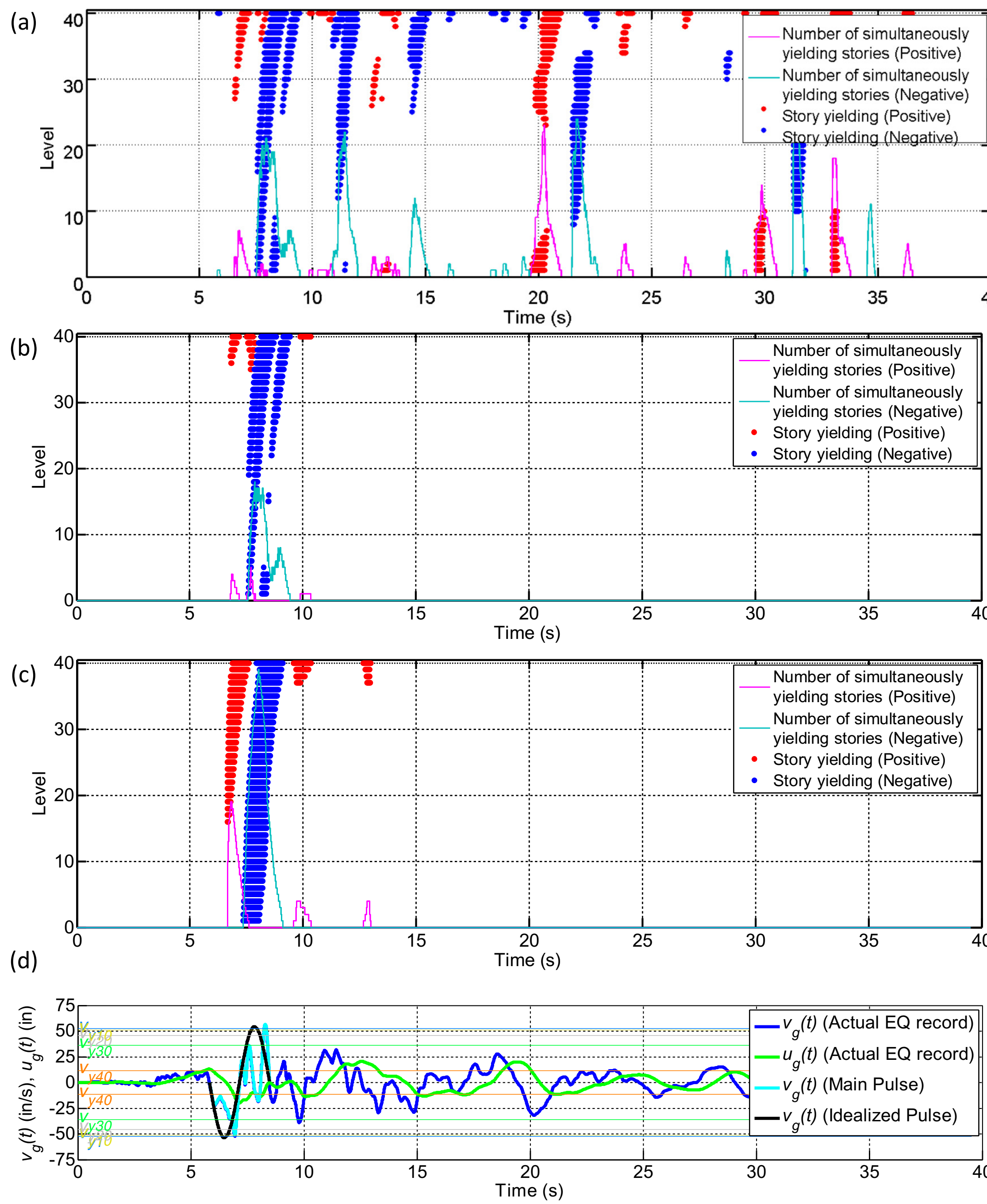

Fig. 12. Story yield time history of Structure-IV subjected to (a) actual earthquake record, (b) isolated main pulse, and (c) main pulse idealized as full-sine velocity pulse, for 1989 Loma Prieta, Hollister Diff. Array (HAD255) earthquake with original time scale.

is presented in the tables for comparison. The $0.5t_d/t_H$ value for each earthquake is also shown for comparison of the number of simultaneously yielding stories to the wavelength of the main pulse.

In the case of original earthquakes (Figs. 14 to 16), since most of the earthquakes have long duration main pulse (indicated by $0.5t_d/t_H$ values larger than 1), simultaneous yielding can be observed in almost all the stories, for those earthquakes. The number of simultaneously yielding stories due to the incident wave predicted using the t_C and t_D curves are found to overestimate the actual yielding (since, the width of the idealized pulse is relatively larger than the actual width of the main pulse of the velocity record, and also because of the long duration pulse, some part of the incident wave gets reflected at the top of the building and interferes with the effects of the incident wave before the entire width of the pulse passes above the base, which is not considered in the estimation procedure for finding the $N_{SYS,Incident}$). The maximum N_{SYS} values obtained using the idealized main pulse is found to provide good prediction of the actual values. Averaging results for the eighteen earthquakes considered, the estimated maximum number of simultaneously yielding stories is found to be 32.2% more than the actual values, with a standard deviation of 35.7%. Since it is challenging to identify the main pulse of earthquake records belonging to the third category (i.e., Category C), and the estimation procedure might not be expected to work as well for this earthquake category, the same average and standard deviation

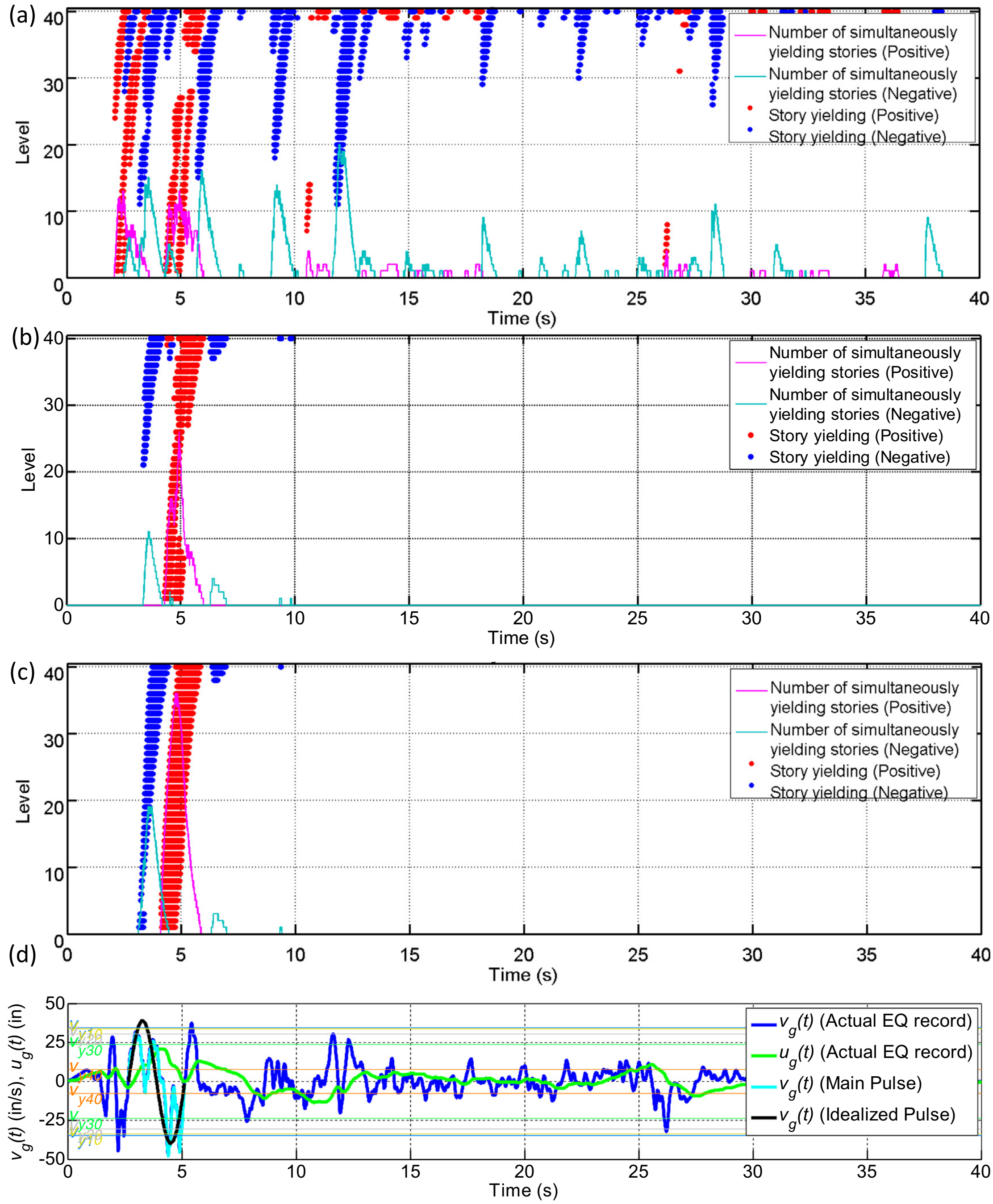

Fig. 13. Story yield time history of Structure-IV subjected to (a) actual earthquake record, (b) isolated main pulse, and (c) main pulse idealized as full-sine velocity pulse, for 1940 Imperial Valley, El Centro Array #9 (I-ELC180) earthquake with original time scale.

were also calculated considering only the first two categories of earthquakes (i.e. Category A and B); the corresponding results are 29.6% and 33.2%, respectively, which is not significantly different from the values obtained considering all earthquake records.

For earthquakes with condensed time scale (Figs. 17 to 19), the main pulse of the earthquakes has short duration with $0.5t_d/t_H$ value equal to 0.39; thus, simultaneous yielding does not occur over all the stories. The number of simultaneously yielding stories due to the incident wave of the main pulse predicted using the t_C and t_D curves have better match with the actual yielding for the earthquakes with condensed times scale, that have shorter duration main pulse, in comparison to the original earthquakes that have long duration main pulse. The maximum number of simultaneously yielding stories occur due to the incident wave and are close to the actual values. Averaging results for the eighteen earthquakes considered, the estimated maximum number of simultaneously yielding stories is 14.7% more than the actual values, with a standard deviation of 22.8%. Again, considering only the first two category of earthquakes (i.e., Category A and B only), the estimated average and standard deviation values are 21.37% and 24% respectively.

In few cases simultaneous yielding occurred at different regions due to closely spaced pulses, however the effects were not found to be significant. Note that each big pulses existing in the earthquake may cause residual deformation and the cumulative effects of the multiple big pulses existing in the earthquake record may cause P-Δ effect. However, since only force based response of the structure is of interest for the study of number of simultaneously

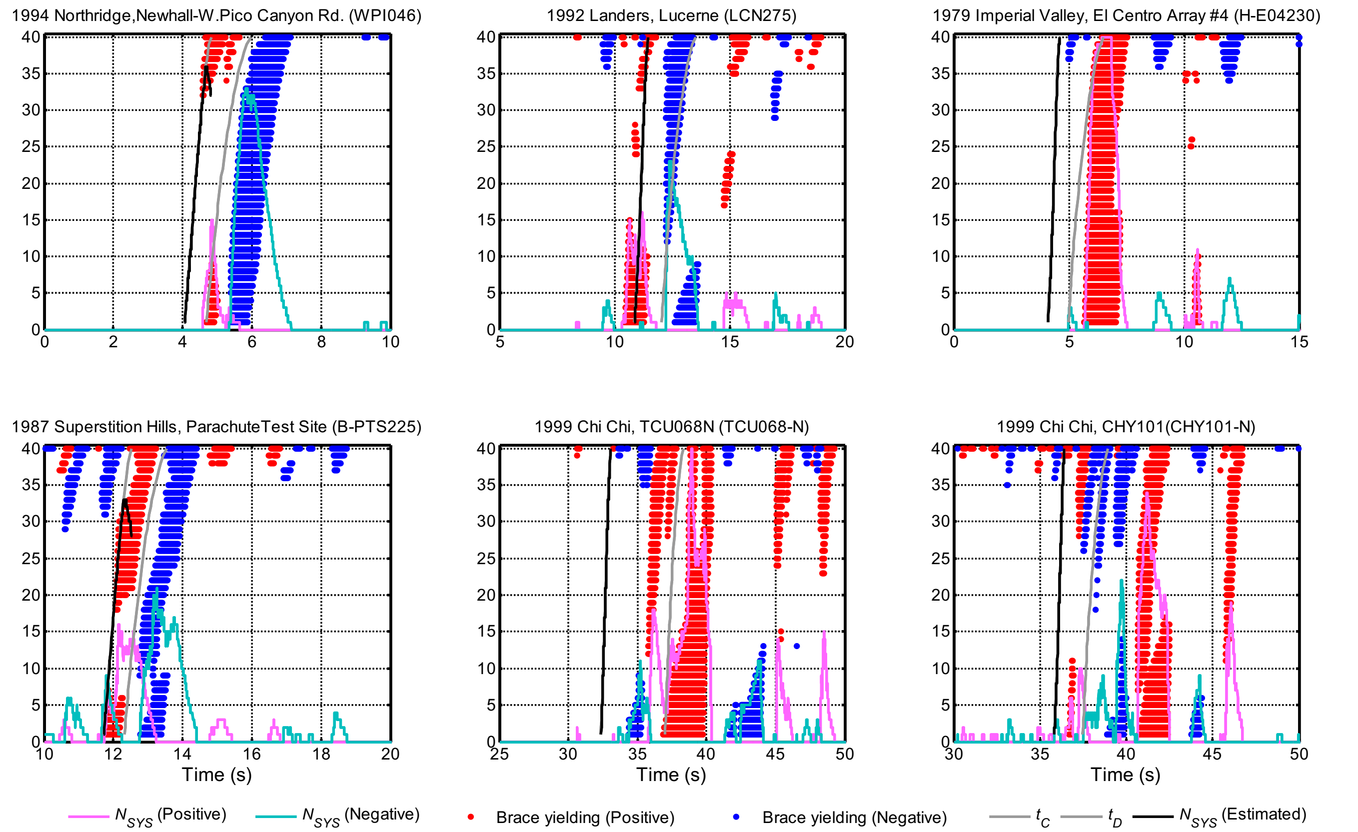

Fig. 14. Story yielding due to the actual earthquake record and due to the incident waves of the idealized main pulse predicted using the t_C and t_D curves for Structure-IV subjected to earthquakes belonging to Category A with original time scale.

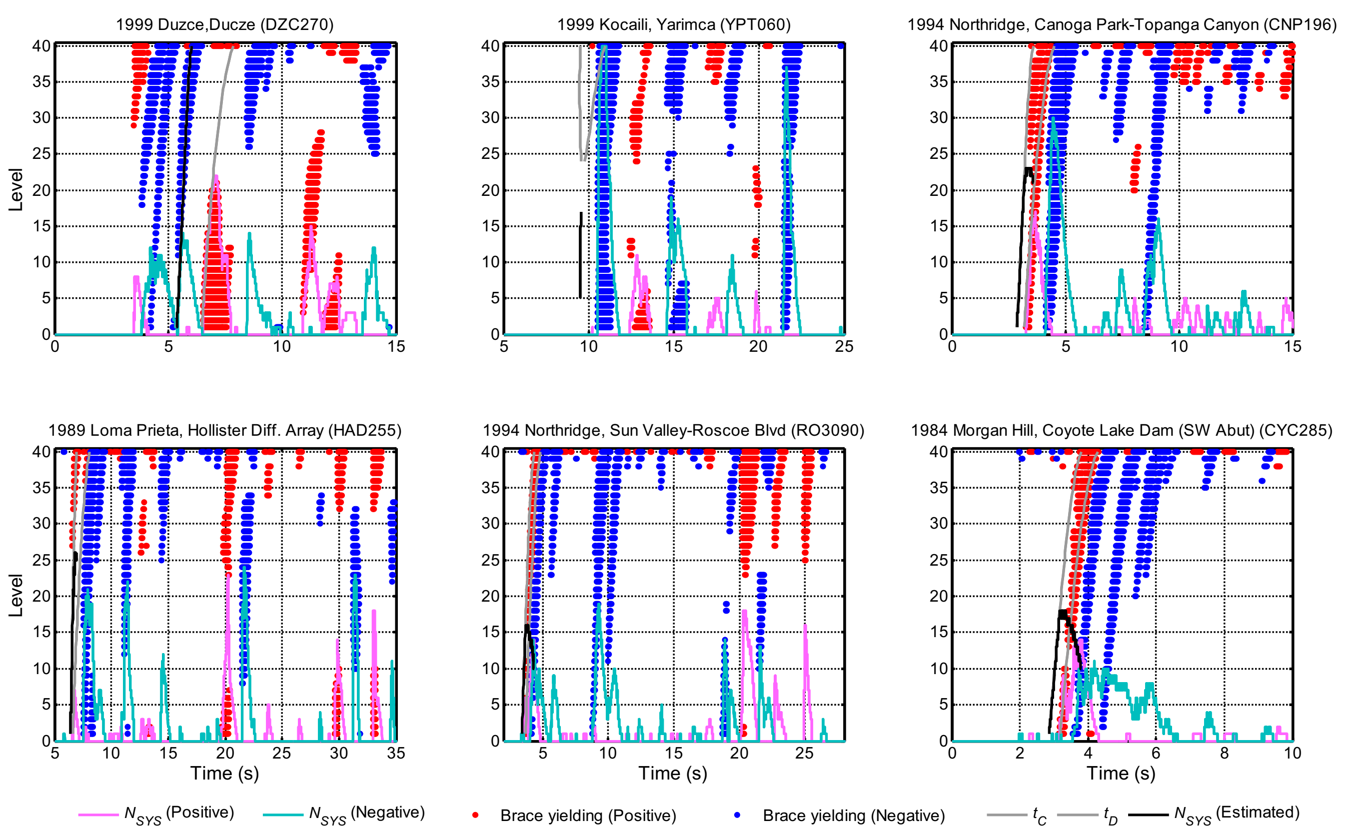

Fig. 15. Story yielding due to the actual earthquake record and due to the incident waves of the idealized main pulse predicted using the t_C and t_D curves for Structure-IV subjected to earthquakes belonging to Category B with original time scale.

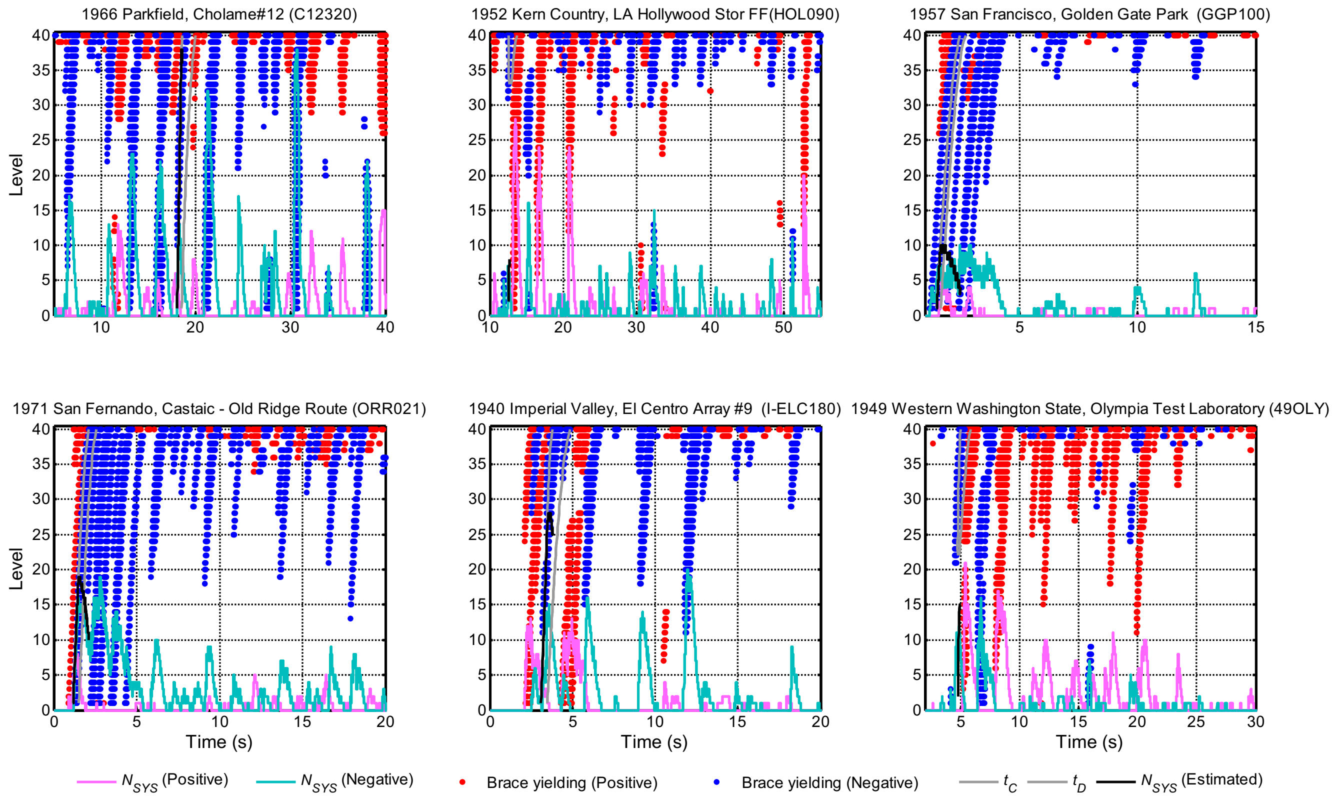

Fig. 16. Story yielding due to the actual earthquake record and due to the incident waves of the idealized main pulse predicted using the t_C and t_D curves for Structure-IV subjected to earthquakes belonging to Category C with original time scale.

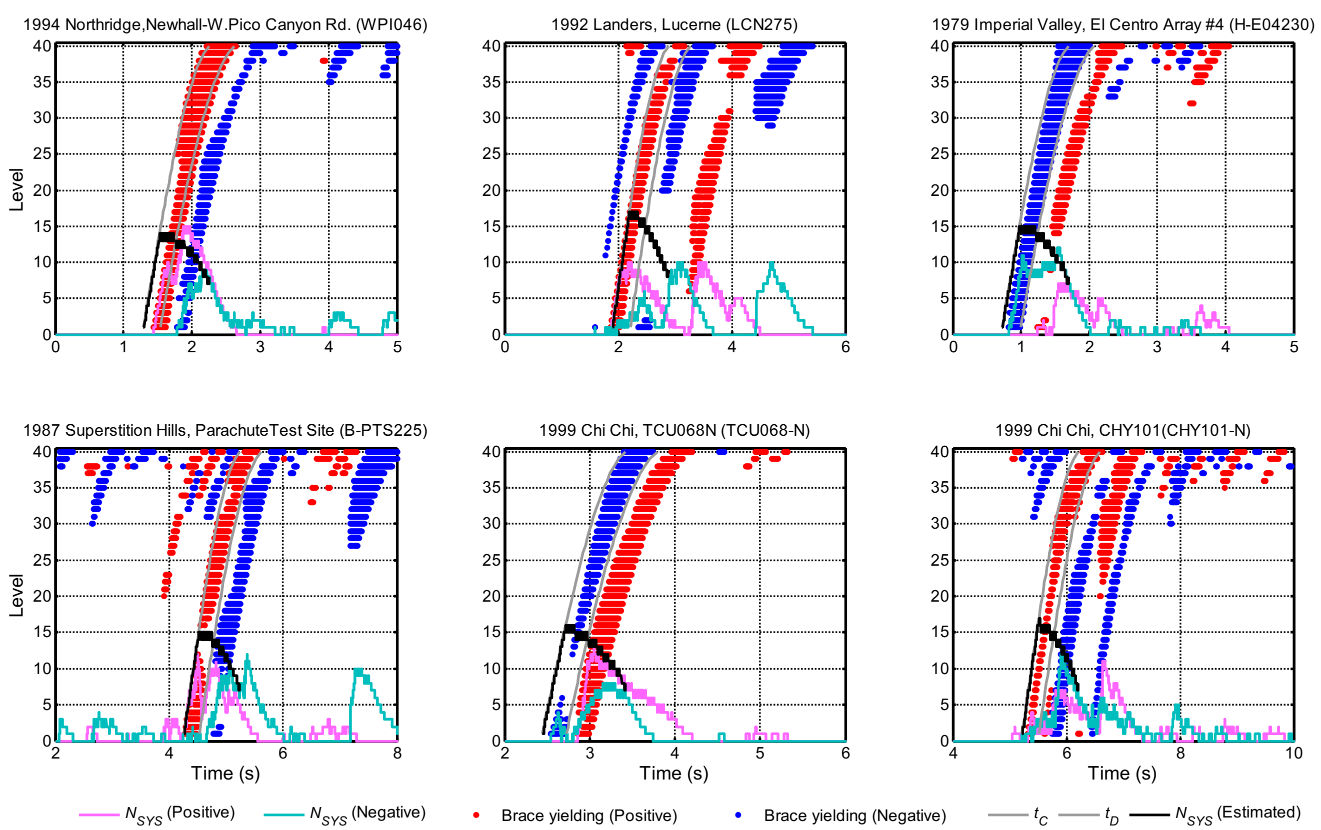

Fig. 17. Story yielding due to the actual earthquake record and due to the incident waves of the idealized main pulse predicted using the t_C and t_D curves for Structure-IV subjected to earthquakes belonging to Category A with condensed time scale.

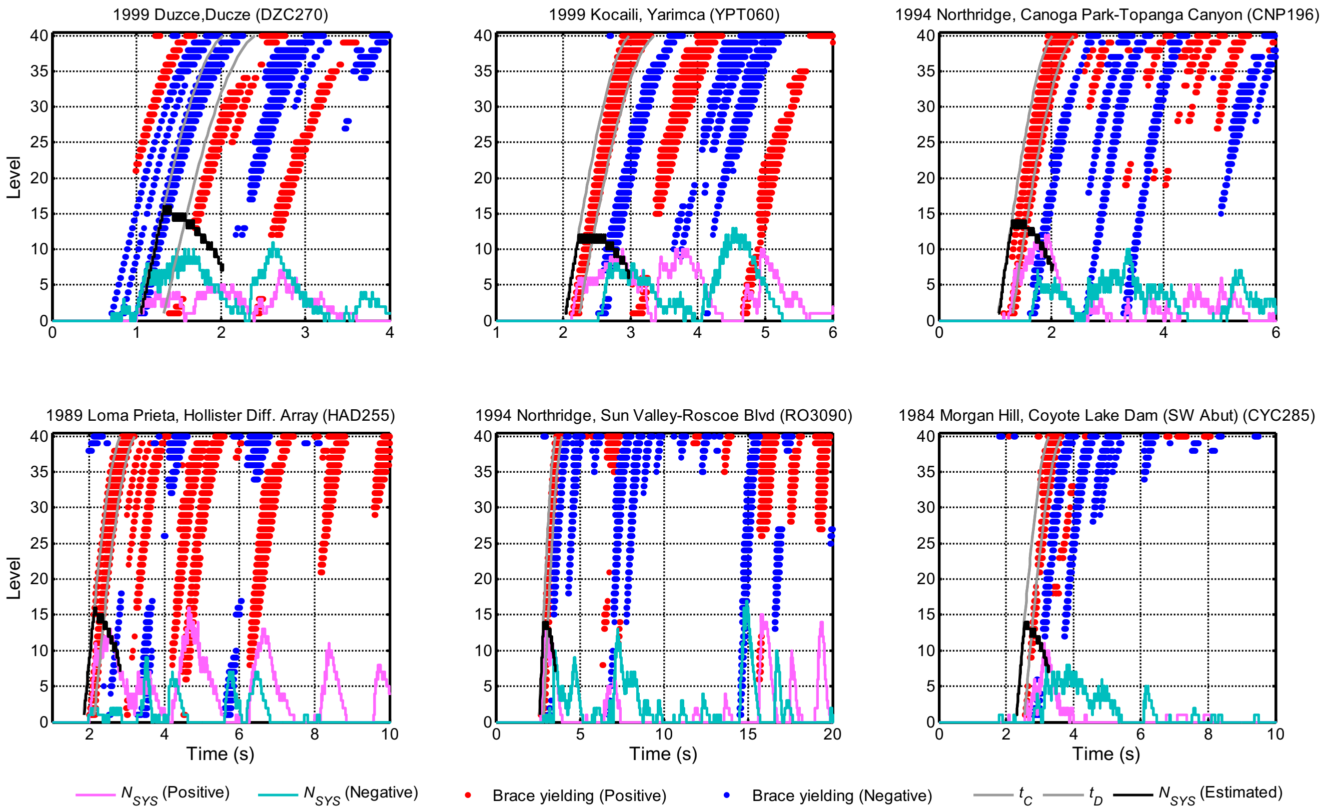

Fig. 18. Story yielding due to the actual earthquake record and due to the incident waves of the idealized main pulse predicted using the t_C and t_D curves for Structure-IV subjected to earthquakes belonging to Category B with condensed time scale.

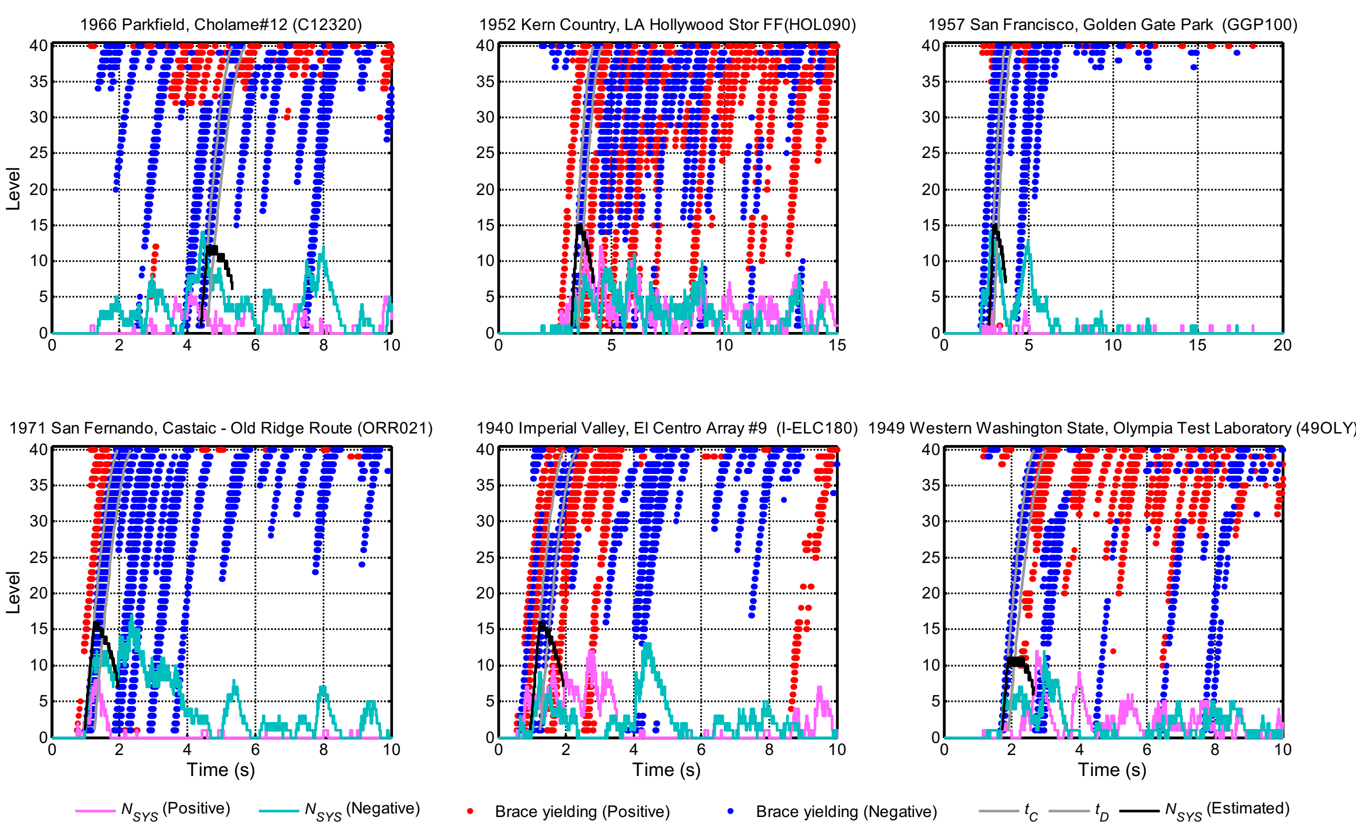

Fig. 19. Story yielding due to the actual earthquake record and due to the incident waves of the idealized main pulse predicted using the t_C and t_D curves for Structure-IV subjected to earthquakes belonging to Category C with condensed time scale.

Table 4
Number of simultaneously yielding stories for Structure-IV subjected to earthquakes with original time scale.

S.N.	Earthquake	$0.5t_d/t_H$	Estimated			Maximum N_{SYS}		Discrepancy %
			$MN_{SYS,Incident}$ (Full-sine)	$N_{SYS,Top}$	$N_{SYS,Base}$	Estimated	Actual	
1	WPI046	1.22	36	40	30	40	33	21.21
2	LCN275	2.2	40	40	40	40	23	73.91
3	H-E04230	2.09	40	40	40	40	40	0
4	B-PTS225	1.07	33	40	27	40	21	90.48
5	TCU068-N	5.25	40	40	40	40	40	0
6	CHY101-N	2.66	40	40	40	40	34	17.65
7	DZC270	1.97	40	40	39	40	28	42.86
8	YPT060	1.7	17	40	37	40	40	0
9	CNP196	1	23	39	26	39	30	30
10	HAD255	1.28	26	40	31	40	24	66.67
11	RO3090	0.51	16	14	14	16	19	-15.79
12	CYC285	0.49	18	13	13	18	14	28.57
13	C12320	1.6	38	40	36	40	38	5.26
14	HOL090	1.4	8	40	33	40	28	42.86
15	GGP100	0.22	10	3	6	10	10	0
16	ORR021	0.47	19	12	13	19	19	0
17	I-ELC180	1.19	28	40	30	40	20	100
18	49Oly	0.96	15	37	25	37	21	76.19
	Considering all earthquakes:							
	Average							32.21
	Standard Deviation							35.68
	Considering Category A and B earthquakes:							
	Average							29.63
	Standard Deviation							33.2

Table 5
Number of simultaneously yielding stories for Structure-IV subjected to earthquake with condensed time scale.

S.N.	Earthquake	$0.5t_d/t_H$	Estimated			Maximum N_{SYS}		Discrepancy %
			$MN_{SYS,Incident}$ (Full-sine)	$N_{SYS,Top}$	$N_{SYS,Base}$	Estimated	Actual	
1	WPI046	0.39	15	9	10	15	15	0
2	LCN275	0.39	17	9	11	17	10	70
3	H-E04230	0.39	15	9	10	15	12	25
4	B-PTS225	0.39	15	9	10	15	12	25
5	TCU068-N	0.39	16	9	10	16	13	23.08
6	CHY101-N	0.39	17	9	10	17	12	41.67
7	DZC270	0.39	16	9	10	16	11	45.45
8	YPT060	0.39	13	9	10	13	13	0
9	CNP196	0.39	14	9	10	14	12	16.67
10	HAD255	0.39	16	9	10	16	16	0
11	RO3090	0.39	14	9	10	14	17	-17.65
12	CYC285	0.39	14	9	10	14	11	27.27
13	C12320	0.39	12	9	10	12	14	−14.29
14	HOL090	0.39	15	9	10	15	14	7.14
15	GGP100	0.39	15	9	10	15	14	7.14
16	ORR021	0.39	16	9	10	16	17	−5.88
17	I-ELC180	0.39	16	9	10	16	13	23.08
18	49Oly	0.39	11	9	10	11	12	−8.33
	Considering all earthquakes:							
	Average							14.74
	Standard Deviation							22.81
	Considering Category A and B earthquakes:							
	Average							21.37
	Standard Deviation							24

yielding stories conducted here, the incremental deformation caused by the pulses do not affect the results. Also note that the building may not be at the initial rest condition at the onset of the main pulse, but this did not seem to have any significant impact on the results. The N_{SYS} values obtained from the procedures proposed here are found to be reasonable.

6. Summary and conclusion

The maximum number of simultaneous yielding stories due to an earthquake was found to be related to the main pulse of the velocity record. When the main pulse of the velocity earthquake record was isolated and idealized with a full-sine velocity pulse, this idealized pulse generated a story yield pattern that resembled the yield pattern corresponding to the main pulse of the actual earthquake record, and the number of simultaneously yielding stories was also close for the two cases. This idealization of the main pulse by an equivalent full-sine pulse enabled the application of a previously proposed procedure by Shrestha and Bruneau [1] for estimating the number of simultaneously yielding stories due to the incident wave of a full-sine velocity base excitation, that uses the t_C and t_D curves representing the beginning and end of story yielding, to estimate the number of simultaneous yielding stories due to the main pulse of the velocity earthquake excitations.

The $N_{SYS,Incident}$ values predicted using those curves were closer to the actual numbers for the earthquakes with condensed time scale in comparison to the earthquakes with original time scale. The predicted maximum N_{SYS} value considering the simultaneous story yielding due to the incident wave and due to the constructive overlapping of the velocity waves obtained by isolating and idealizing the main pulse of the velocity base excitation were reasonably close to the maximum N_{SYS} value obtained for the main pulse of the actual earthquake. For earthquakes with original time scale, averaging the results for the eighteen earthquakes considered, the estimated maximum number of simultaneously yielding stories was 32.2% more than the actual values with a standard deviation of 35.7%. For the same earthquake but having a condensed time scale, on average, the estimated maximum number of simultaneously yielding stories was 14.7% more than the actual values, with a standard deviation of 22.8%.

The main findings of the study are enumerated as follows:

1. The maximum number of simultaneously yielding stories was found to be related to the main pulse in the earthquake velocity record.
2. The systematic procedure of identifying the dominant pulse of an earthquake record was found to give good results for most of the earthquakes, especially the pulse-type earthquakes.
3. Use of full-sine velocity pulse to idealize the main pulse of the building could adequately resemble the story yield pattern and the number of simultaneously yielding stories as observed due to the main pulse of the earthquake record.
4. The method for estimating the number of simultaneously yielding stories, using equations developed for the t_C and t_D curves obtained by considering a full-sine velocity pulse, provided satisfactory estimates of the number of story yielding caused by the main pulse of the earthquake record.

Hence, the proposed procedure for estimating the number of simultaneously yielding stories due to an earthquake, that consists of isolating and idealizing the main pulse by a full-sine velocity pulse and using the estimation procedure developed for the full-sine velocity base excitation, was found to provide satisfactory and conservative results.

7. Future research

This study could be further continued to formulate a procedure for calculating the axial force demands by incorporating the force transferred from the simultaneously yielding stories caused by the incident wave and due to the overlapping of the incident and the reflected waves occurring at the top and bottom of the building, as predicted from the procedures developed here, along with the forces from the non-yielding stories. Thereafter, future research can investigate how the study can further be extended to include flexural behavior that exists in tall structures and address issues related to more complicated structures; this would include application of the estimation procedure on lateral-force resisting frames such as EBF and BRBF.

Acknowledgements

This research was partly supported by the MCEER (Multidisciplinary Center for Earthquake Engineering Research) at the University at Buffalo. Any opinions, findings, conclusions, or recommendations in this paper, however, are solely of the authors and do not necessarily reflect the views of the sponsors.

References

[1] Shrestha L, Bruneau M. Estimating number of simultaneously yielding stories in a shear building subjected to full-sine pulse velocity base excitation. Eng Struct 2017;134:236–52.
[2] Hall JF, Heaton TH, Halling MW, Wald DJ. Near-source ground motion and its effects on flexible buildings. Earthquake Spectra 1995;11(4):569–605.
[3] Bruneau M, Wang N. Some aspects of energy methods for the inelastic seismic response of ductile SDOF structures. Eng Struct 1996;18(1):1–12.
[4] Bruneau M, Wang N. Normalized energy-based methods to predict the seismic ductile response of SDOF structures. Eng Struct 1996;18(1):13–28.
[5] Mavroeidis GP, Papageorgiou AS. A mathematical representation of near-fault ground motions. Bull Seismol Soc Am 2003;93(3):1099–131.
[6] Baker JW. Quantitative classification of near-fault ground motions using wavelet analysis. Bull Seismol Soc Am 2007;97(5):1486–501.
[7] Vassiliou MF, Makris N. Estimating time scales and length scales in pulselike earthquake acceleration records with wavelet analysis. Bull Seismol Soc Am 2011;101(2):596–618.
[8] Kalkan E, Kunnath SK. Effects of fling step and forward directivity on seismic response of buildings. Earthquake Spectra 2006;22(2):367–90.
[9] Krishnan S, Muto M. Mechanism of collapse of tall steel moment-frame buildings under earthquake excitation. J Struct Eng 2012;138(11):1361–87.
[10] Shrestha L, Bruneau M. Seismic Demand in Columns of Steel Frames, Technical Report MCEER-16-0002. MCEER: University at Buffalo, Buffalo, NY; 2016.